

UNIVERSITA' DEGLI STUDI DI MILANO

Facoltà di Agraria

Dipartimento di Scienze Molecolari Agroalimentari

Scuola di Dottorato in Scienze biochimiche, nutrizionali e metaboliche

Dottorato di Ricerca in Biochimica, XXI ciclo, BIO/10



UNRAVELLING FUNCTIONAL INTERACTIONS OF THE RHODANESE- LIKE PROTEIN RhdA OF *AZOTOBACTER VINELANDII*

Tutor: Chiar.ma Prof.ssa Silvia PAGANI

Coordinatore: Chiar.ma Prof.ssa Silvia PAGANI

Tesi di Dottorato di Ricerca di:

Dr.ssa Francesca CARTINI

Matr. N. R06566

Anno Accademico 2007-2008

TABLE OF CONTENTS

1 INTRODUCTION	1
1.1 Rhodanese homology domain proteins	2
1.2 <i>Azotobacter vinelandii</i> RhdA and <i>Escherichia coli</i> SseA: the prototypes of two-domains rhodanese-like proteins	6
1.2.1 Peculiarity of <i>A. vinelandii</i> RhdA	11
1.2.2 <i>E. coli</i> SseA: a prototype of prokaryotic MST enzyme	12
1.3 Sulfur mobilization: the role of cysteine desulfurases	14
1.4 The importance of persulfidic sulfur	18
2 AIM	20
3 RESULTS	22
3.1 Details of sulfane sulfur transfer from <i>E. coli</i> IscS to RhdA	23
3.2 Expression and purification of <i>A. vinelandii</i> cysteine desulfurase	27
3.3 Sulfane sulfur transfer between <i>A. vinelandii</i> cysteine desulfurase and RhdA	29
3.4 Effects of RhdA on the activity of the <i>A. vinelandii</i> cysteine desulfurases NifS and IscS	32
3.5 Searching protein-protein interactions	35
3.6 Phenotypic difference between <i>E. coli</i> Δ sseA6 and <i>A. vinelandii</i> Δ rhdA	39
3.6.1 Effects of <i>rhdA</i> deletion on <i>A. vinelandii</i> growth	40
3.6.2 Effects of <i>sseA</i> deletion on <i>E. coli</i> growth	42
3.6.3 Effects of <i>sseA</i> deletion on <i>E. coli</i> growth in condition mimicking oxidative stress	43
4 Concluding remarks	48

5. Materials and methods	51
5.1 Strains, media and bacterial cultures	52
5.1.1 Plasmid vectors	53
5.1.2 BL21(DE3) transformation	54
5.1.3 Protein overexpression in <i>E.coli</i>	54
5.2 Preparation of bacterial extracts and purification of the over-expressed proteins	55
5.2.1 <i>A. vinelandii</i> total protein extract	55
5.2.2 RhdA purification	55
5.2.3 <i>A. vinelandii</i> cysteine desulfurases purification	56
5.3 Enzyme assay	57
5.3.1 Thiosulfate:cyanide sulfurtransferase (TST) activity	57
5.3.2 Cysteine desulfurase activity assays	57
5.3.2.1 Alanine production	57
5.3.2.2 Sulfane sulfur determination	58
5.4 Spectroscopic measurements	59
5.5 Protein-protein interactions	60
5.5.1 Size-exclusion chromatography	60
5.5.2 Immunoaffinity chromatography	60
5.6 Protein electrophoresis	62
6 References	63

1.Introduction

1.1 Rhodanese homology domain proteins

The complete sequencing of more than 860 genomes (<http://www.genomesonline.org/gold.cgi?want=Published+Complete+Genomes>) has shown that proteins bearing sequence similarity to bovine rhodanese (thiosulfate:cyanide sulfurtransferase, TST) are widely distributed among all living organisms.

Rhodanases (TSTs) *in vitro* catalyze the transfer of a sulfur atom from thiosulfate to cyanide, with concomitant formation of thiocyanate (Fig.1) (Westley, 1977).

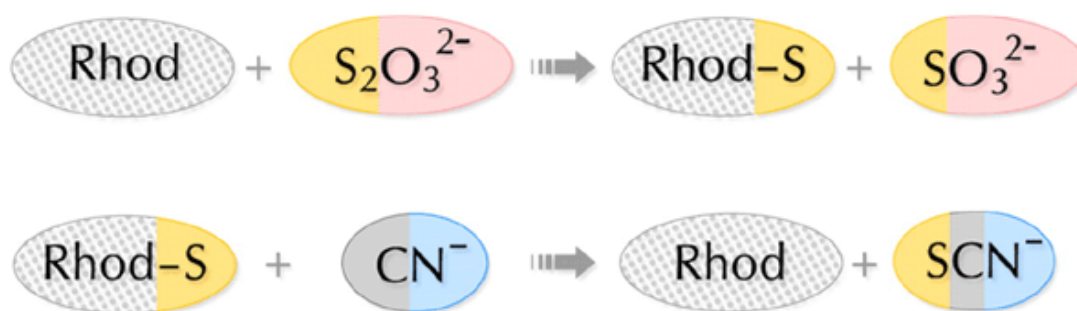


Figure 1. Scheme representing the sulfur-transfer reaction catalyzed by rhodanese.

The most well characterized TST is bovine liver rhodanese (Rhobov) that is composed of two identically folded domains of about 120 amino acids long (Ploegman *et al.*, 1978), which display weak sequence similarity to one another (13 and 21% identical residues, respectively). Due to this peculiar tandem domain architecture, bovine rhodanese has been considered the prototype of divergent evolution from a common ancestor protein which, after gene duplication and under the constraint of tertiary structure conservation, led to the almost complete obliteration of sequence similarity between the two domains (Bordo *et al.* 2002). Only the C-terminal domain (referred to as the catalytic domain) hosts the catalytic Cys residue, which is the first residue of a six amino-acid active-site loop that folds in a cradle-like structure defining the enzyme catalytic pocket.

The recent biochemical and structural characterization of GlpE, a single rhodanese domain TST from *Escherichia coli* (Ray *et al.*, 2000; Spallarossa *et al.*, 2001), indicates that the catalytically inactive N-terminal domain found in tandem domain rhodanese-like proteins is not essential for catalysis.

Sensitive homology search programs based on profile analysis or Hidden Markov Models have detected rhodanese homology domains coded by 500 genes in the three major evolutionary phyla (see, for example, SMART, <http://smart.embl-heidelberg.de>; DART, <http://www.ncbi.nlm.nih.gov/Structure/cdd/cdd.shtml>). Often, distinct proteins containing rhodanese domains are encoded in the same genome. In the human genome, 47 such instances are observed, in the *Escherichia coli* K12 genome, nine rhodanese-like proteins are found (Blattner *et al.*, 1997; Tatusov *et al.* 2000). From a structural viewpoint, rhodanese-like proteins are either composed of two rhodanese domains, with the C-terminal domain displaying the putative catalytic Cys as observed in Rhobov and RhdA, the rhodanese-like protein from *Azotobacter vinelandii* (Colnaghi *et al.* 1996), or composed of a single catalytic rhodanese domain, as found in GlpE (Ray *et al.*, 2000; Spallarossa *et al.*, 2001). Rhodanese domains, either catalytic or inactive (i.e. where the active-site Cys is replaced by another residue), are also found associated with other protein domains such as MAPK-phosphatases (Keyse *et al.*, 1993; Fauman *et al.*, 1998; Hofmann *et al.*, 1998) or Thil, an *E. coli* enzyme involved in thiamin and thiouridine biosynthesis (Palenchar *et al.*, 2000).

A multiple alignment of the rhodanese homology domain, containing a representative subset of the entries detected in the genomic database, is provided by the SMART resource (Schultz *et al.*, 1998). The deduced neighbour-joining (N-J) tree provides a graphical representation of the mutual similarity among distinct amino-acid sequences (Fig.2, Bordo *et al.* 2002).

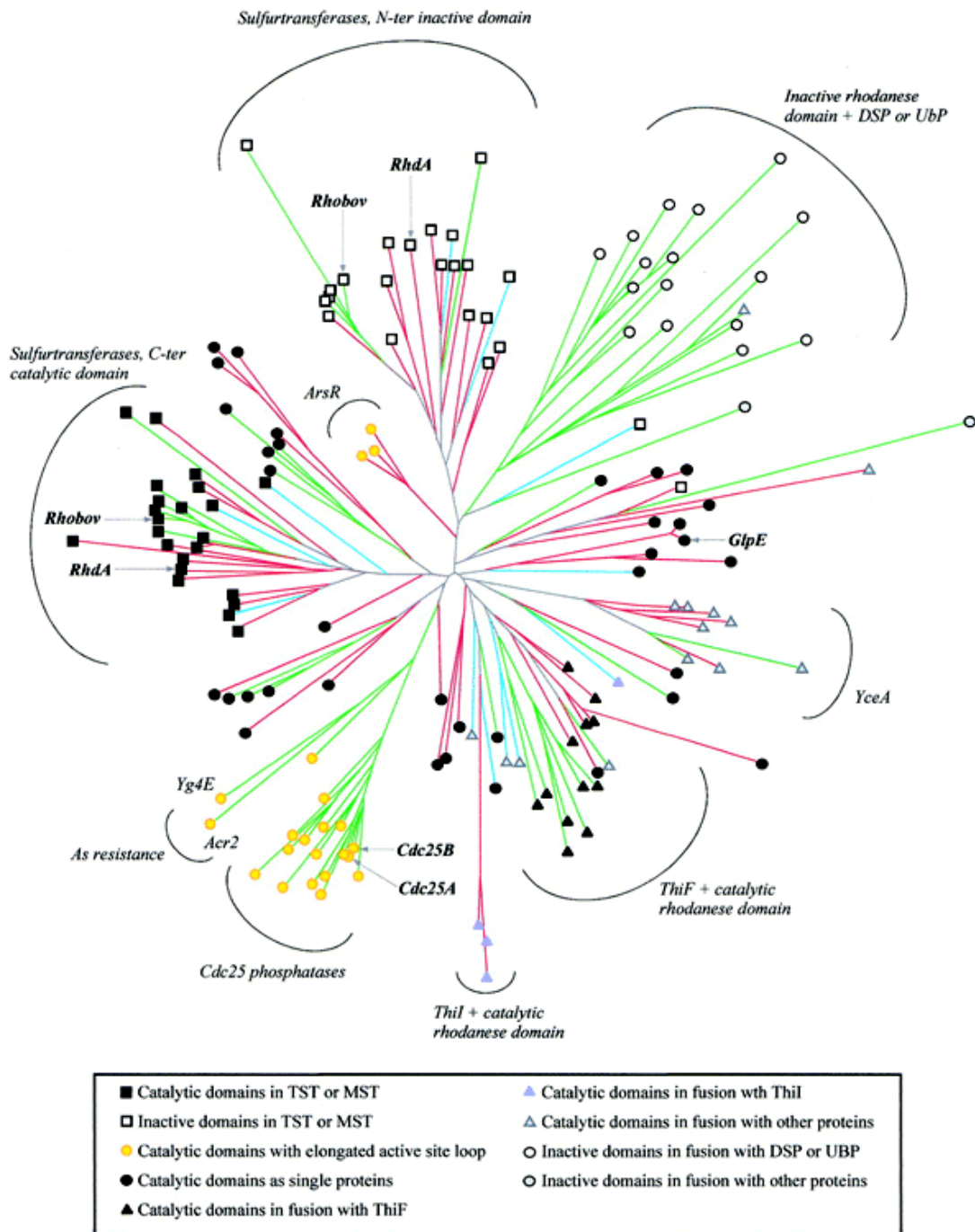


Figure 2. Neighbour-joining tree representing the rhodanese superfamily generated by CLUSTALW (correction for multiple substitution was adopted; Thompson *et al.*, 1997). The multiple alignment was derived from that included in the SMART resource, to which four *E. coli*, two archaea and two ThiI proteins were added, for a total of 155 rhodanese modules. The SMART alignment represents an even sample of the total number of rhodanese modules, as closely related sequences are represented only once. The tree was displayed and validated by bootstrap analysis using programs in the PHYLIP package (Felsenstein, 1989). Archaeal, bacterial and eukaryotic proteins are represented in blue, red and green, respectively. Symbols

are used to indicate the distinct structural or functional roles of the rhodanese modules, as described in the inset.

The N- and C-terminal domains of rhodanese superfamily form two distinct subfamilies that include thiosulfate-cyanide (TST) and mercaptopyruvate-cyanide (MST) sulfurtransferases, (Nagahara *et al.*, 1995-1996; Papenbrock *et al.*, 2000; Colnaghi *et al.*, 2001). Notably, active-site loop amino-acid sequences are distinct in TSTs and in MSTs, displaying the motifs CRXGX[R/T] and CG[S/T]GVT, respectively (square brackets indicate alternative residues, 'X' any amino acid; Fig.3). The active-site loop of known TSTs always contains two basic residues (i.e. if the last loop residue is Thr, a basic residue is observed at one of the X positions), whereas no charged residues are observed in biochemically characterized MSTs. This structural feature may be related to the distinct ionic charge of the respective *in vitro* substrates, thiosulfate (2⁻) and 3-mercaptopyruvate (1⁻).



Modules	Active site loop motif	Specie distribution
Thiosulfate:cyanide sulfurtransferases (TST) 	CRXGX[R/T]	Eukaryota Bacteria Archaea
3-mercaptopyruvate sulfurtransferases (MST) 	CG[S/T]GVT	Eukaryota Bacteria

Figure 3. Rhodanese modules: domains are schematized as coloured boxes. Catalytic rhodanese modules with a six amino-acid active-site loop are shown in red, and inactive rhodanese modules are displayed in black.

1.2 *Azotobacter vinelandii* RhdA and *Escherichia coli* SseA: the prototypes of two-domains rhodanese-like proteins.

As before stated, in the majority of organisms, the proteins of the rhodanese homology superfamily ([Accession No.: PF00581; http://www.sanger.ac.uk/Software/Pfam/](http://www.sanger.ac.uk/Software/Pfam/)) are present as paralogs, thus corroborating the hypothesis of their distinct biological roles other than cyanide scavengers. The emerging picture by “*in silico*” analyses (Bordo *et al.*, 2002), however, points to a role of the active-site structure of rhodanases in substrate recognition.

RhdA and SseA are representative prototypes of tandem-domains rhodanese proteins (Bordo *et al.*, 2000), belonging to two different subfamilies: TSTs and MSTs, respectively.

A. vinelandii RhdA (Colnaghi *et al.*, 1996; Bordo *et al.*, 2001; Pagani *et al.*, 2000) was classified as a TST on the basis of its ability to catalyze the typical *in vitro* rhodanese reactions.

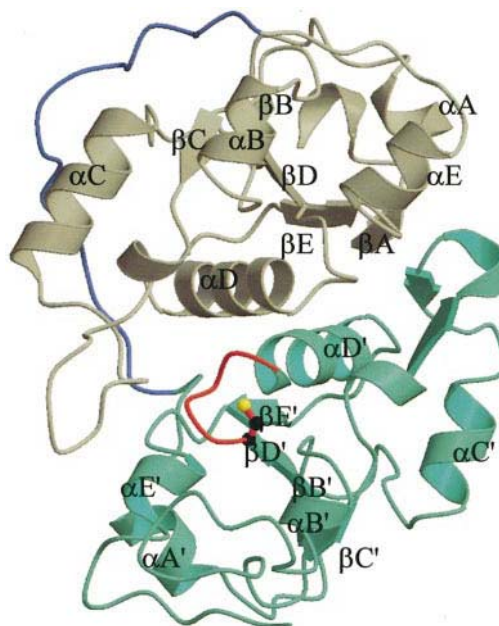


Figure 4. Ribbon representation of RhdA. The N- and C-terminal domains (brown and green, respectively), the linker peptide (blue), (Bordo *et al.*, 2000). A single quote indicates elements of

the C-terminal domains. The active-site loop is shown in red; the catalytic residue, Cys₂₃₀, is represented in ball and stick.

The enzyme molecule is composed of two similarly folded α/β domains, each of approximately 125 amino acids (Fig. 4), displaying very similar three-dimensional structure, both contain a central parallel β -sheet surrounded by α -helices. A trace of the ancestral gene duplication is still present in the amino acid sequence of the two RhdA domains, which have 26 identical residues out of a total of 125 (20.8 %).

The active-site residue, Cys₂₃₀, the only Cys present in the whole protein, is located in the C-terminal domain at the bottom of a shallow round pocket on the protein surface. The active-site loop adopts a semicircular, cradle-like, conformation, which allows precise positioning of the Cys₂₃₀ S atom at the bottom and in the centre of the active-site pocket (Fig. 5).

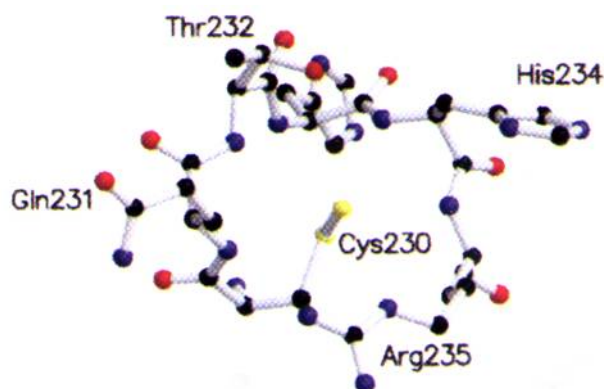


Figure 5. *A. vinelandii* RhdA catalytic loop (CQTHHR)

The RhdA catalytic centre has a structure (HCQTHHR) not commonly found in rhodanese-like proteins that originates a strong positive electrostatic field, thus favouring stabilization of a persulfide bond on the catalytic Cys₂₃₀ residue. This feature is due to the six peptide dipoles, from 230 to 235, radially oriented with their positive ends aiming at the centre of the catalytic pocket, thus making an active site with electrostatic and sterical properties of an anion binding site.

The *E. coli* *sseA* gene (Hama *et al.*, 1994) is considered as a reference for 'sseA Cluster of Orthologous Groups' (COG 2897, <http://www.ncbi.nlm.nih.gov/COG>) containing genes encoding proteins with both 'rhodanese signatures'. *E. coli* *sseA* encodes for a 31 kDa protein, which is endowed with 3-mercaptopyruvate-dependent sulfurtransferase activity (Colnaghi *et al.*, 2001). SseA displays clear sequence similarity to RhdA: 27% identical residues, including the conservation of the active site Cys (Cys₂₃₇), which is the only Cys residue in SseA.

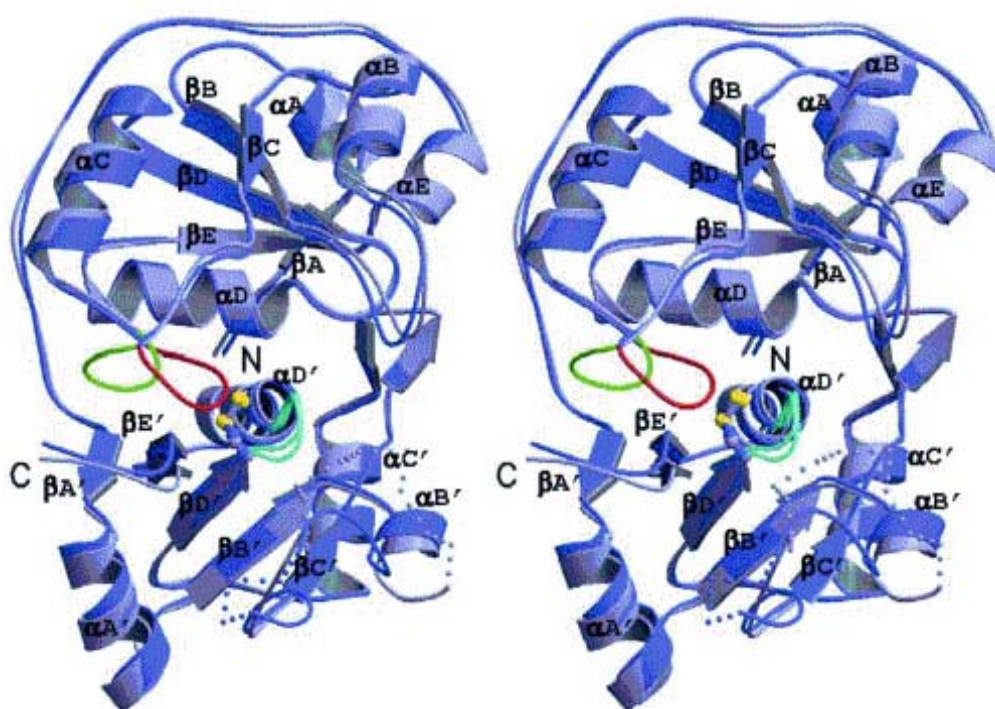


Figure 6: Stereo view of the two SseA molecules in the asymmetric unit. Molecules A and B are displayed as ribbon diagrams. A single quote indicates elements of the C-terminal domains. The closed and open conformations adopted by the 61–67 segment in molecules A and B are displayed in red and green, respectively. Active site loops are shown in cyan and the catalytic residue, Cys₂₃₇, is depicted in ball-and-stick. The portion of $\alpha B'$ – $\beta C'$ loops which are disordered in both SseA molecules are represented as dotted lines; their position is purely hypothetical. The drawings were prepared with the programs MOLSCRIPT (Kraulis *et al.*, 1991) and Raster3D. (Merrit *et al.*, 1994).

The SseA overall tertiary structure conforms to that observed in the tandem-domains rhodanese proteins, Rhobov and RhdA (Ploegman *et al.*, 1978;

Bordo *et al.*, 2000) with some significant variation of the active site environment, with possible implications for the catalytic mechanism. In SseA, the two rhodanese domains are composed of approximately 130 amino acids each (Fig. 6) structured to form a central parallel β -sheet bordered by α -helices, (Spallarossa *et al.*, 2004).

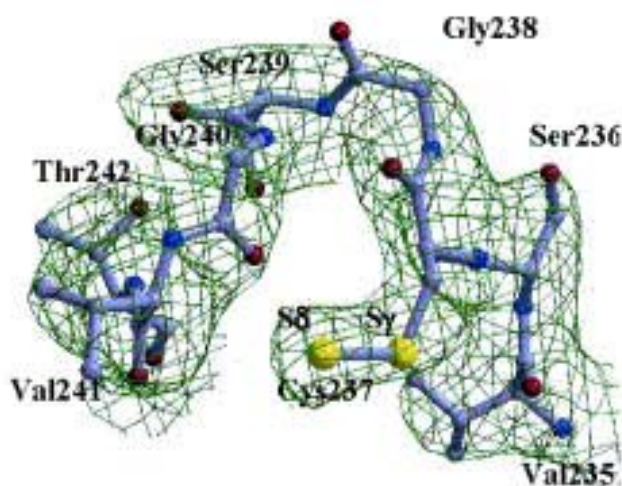


Figure 7: Active site region of the SseA molecule. C, N, O and S atoms are shown in grey, blue, red and yellow, respectively. The picture was drawn with the program MOLSCRIPT, (Esnouf, 1997).

In SseA, the catalytic Cys is the first residue in a six residue loop (CGSGVT), (Fig.7). Remarkably, in spite of the homology and overall structural similarity with RhdA, the SseA active site loop conformation is different from that found in RhdA. The two distinct conformations adopted by the amino acid residues 61–67, “closed” and “open”, affect both the solvent accessibility and the structural neighbourhood of the active Cys residue (Fig.8). In the closed conformation, the β C– α C loop displays a structure similar to that observed in RhdA, fully burying the Cys₂₃₇ side-chain in the protein core. In the open conformation, a shallow cleft is formed by residues His₆₆, Met₆₇, Arg₁₀₂, Gly₂₄₀, Val₂₄₁ and Asp₂₆₂ (Fig.8), exposing to solvent the Cys₂₃₇ S atom, suggesting the involvement of these residues in the catalytic mechanism. In fact, Arg₁₀₂ is the only positively charged residue available for anchoring the 3-mercaptopyruvate, orienting the substrate 3-thiol group towards Cys₂₃₇, at

the onset of the catalytic cycle. According to that, His₆₆ and Arg₁₀₂ would act as key residues for substrate recognition and orientation. Cys₂₃₇ and Asp₂₆₂, in view of their nucleophilic character, would play an essential and active role in the recognition of the sulfur donor. Notably, these four residues are well conserved in all known MSTs.

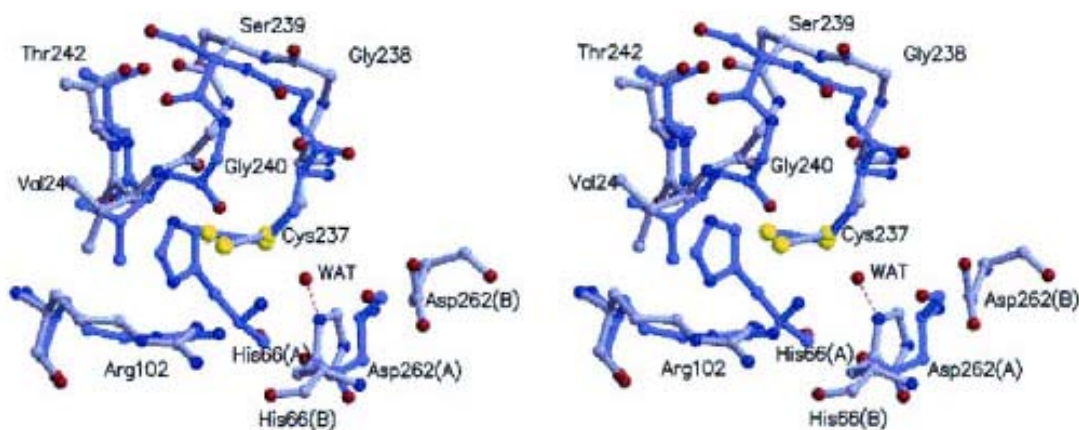


Figure 8: Overlay of the two active site loops (A closed; B open), highlighting the different conformations achieved as a consequence of the 61–67 segment shift.

The above observations suggest that shifting of the 61–67 loop may be a structural factor related to SseA functionality: binding of the sulfur donor could promote further structural changes in the active site, enhancing accessibility to the reactive Cys. In this respect, it should be noted that active site reshaping in SseA is opposed to active site rigidity observed in TSTs, where the catalytic Cys residue does not require conformational transitions (Ploegman *et al.*, 1978; Bordo *et al.*, 2000). Such differences may provide the structural bases for the specific catalytic mechanisms which distinguish TSTs from MSTs. In the reference TST Rhobov, a ping-pong mechanism is observed and the reaction proceeds *via* the formation of a stable persulfurated intermediate (Westley *et al.*, 1983). In rat liver MST, the reaction proceeds through a sequential mechanism, whereby the donated sulfur atom is directly transferred to the sulfur acceptor, assisted by the catalytic Cys residue (Nagahara *et al.*, 1999).

The strong conservation of the active site loop CG[S/T]GVT sequence motif, within the MST family, suggests that such a motif is instrumental for achieving the twisted active site conformation observed in SseA.

1.2.1 Peculiarity of *A. vinelandii* RhdA

As before stated, the RhdA active-site motif (HCQTHHR) is not currently found in rhodanese domain proteins. In RhdA, conserved catalytic cysteine is surrounded by residues that are entirely different from those found in the vertebrate enzymes (Colnaghi *et al.*, 1996; Bordo *et al.*, 1999). In the active site motif of the bovine rhodanese (Ploegman *et al.*, 1978), the cationic residue Lys₂₄₉ has been identified as catalytic requirement for the sulfur transfer function (Luo *et al.*, 1994) and replacement of Lys₂₄₉ with an hydrophobic residue (Ala) knocks out Rhobov ability to transfer sulfane sulfur *in vitro*. In RhdA, the corresponding residue is Thr₂₃₂. When Thr₂₃₂ was replaced with either Lys or Ala (Pagani *et al.* 2000), the ability to transfer sulfane sulfur from thiosulfate to cyanide increased about three-fold in both mutants as compared to that of the wild-type RhdA (Pagani *et al.* 2000). This result evidenced that the catalytic proprieties of RhdA are different from those of known TSTs.

Furthermore, the inspection of the RhdA active-site 3D structure (Bordo *et al.*, 2000-2001) highlighted the structural relationship with the active-site structures of Cdc25 phosphatases (Fauman *et al.*, 1998; Reynolds *et al.*, 1999). In Cdc25 phosphatases the active site loop [His–Cys–(X)₅–Arg] is one residue longer than in RhdA [His–Cys–(X)₄–Arg]. To prove the hypothesis that the length of the RhdA active-site loop should play a key role in substrate recognition and catalytic activity, RhdA scaffold was the starting point for producing mutants with single-residue insertion to generate the catalytic loop HCQTHAHR and HCQTHSHR. Analyses of the catalytic performances of these engineered RhdAs revealed that elongation of the catalytic loop definitely compromised the ability to catalyze sulfur transfer reactions, while it

generated the ability to hydrolyze phosphorus-containing compounds, (Forlani *et al.*, 2003).

Another peculiar feature of RhdA is that, after heterologous expression in *E.coli*, RhdA is purified in a mixture of persulfurated and unpersulfurated forms, and L-cysteine was identified as the most effective sulfur source in producing RhdA-SSH (Forlani *et al.*, 2005).

As before stated, the active-site loop of RhdA appears properly designed to stabilize its persulfurated form (RhdA-SSH), and RhdA-SSH was productively used as the only sulfur source for in vitro 2Fe-2S cluster assembly in apo-adrenodoxin (Cereda *et al.*, 2003).

1.2.2 *E. coli* SseA, a prototype of prokaryotic MST enzyme

SseA is the first identified prokaryotic tandem-domain rhodanese protein with a preference for 3-mercaptopyruvate over thiosulfate as substrate (Colnaghi *et al.*, 2001).

The phylogenetic relation between eukaryotic TSTs and MSTs was claimed (Nagahara *et al.*, 1995), and the sequence stretch around the catalytic Cys is considered a key motif for the preference of 3-mercaptopyruvate or thiosulfate as sulfur donor substrates (Nagahara *et al.*, 1995, 1996, 1999). The pioneering work of Luo and Horowitz (Luo *et al.*, 1994) identified the lysine residue (at the position +2 with respect to the catalytic Cys) as key amino acid for binding and catalysis of thiosulfate in bovine rhodanese. The SseA preference for 3-mercaptopyruvate over thiosulfate as donor substrate corroborates the critical role in the substrate selection of the amino acid residues just behind the catalytic Cys. Mutagenic analysis (Colnaghi *et al.*, 2001) of Ser₂₄₀ of SseA provided further evidence that the presence of a hydrophobic residue (Ala) did not affect the binding of 3-mercaptopyruvate, but strongly prevented thiosulfate binding. On the contrary, the presence of a positively charged residue (Lys) significantly increased the affinity for thiosulfate. As already suggested for rat MST (Nagahara *et al.*, 1996, 1999),

the interaction with 3-mercaptopyruvate should be favoured by other ionisable residues likely close to the catalytic cysteine in the three-dimensional structure of the catalytic pocket. A rationale for this is provided by the 3D structure of SseA. Location of the SseA catalytic Cys₂₃₇ residue suggests the involvement of the conserved Arg₁₀₂ in orienting and stabilizing the substrate in the active site, (Spallarossa *et al.*, 2004). In SseA, Arg₁₀₂ is the only positively charged residue available for anchoring and orienting the 3-mercaptopyruvate towards Cys₂₃₇, and His₆₆ and Arg₁₀₂ would act as key residues for substrate recognition and orientation. Cys₂₃₇ and Asp₂₆₂, in view of their nucleophilic character, would play an essential and active role in the catalytic mechanism. Notably, these four residues are well conserved in all known MSTs.

The preference for 3-mercaptopyruvate over thiosulfate as sulfur donor, inferred by the *in vitro* activity behaviours of SseA, and the findings obtained by mutagenic analysis, confirmed that the active-site loop sequence CGSGVTA can be taken as discriminative motif for MST also in prokaryotic enzymes.

1.3 Sulfur mobilization: the role of cysteine desulfurases

Cysteine has been shown to be the source of sulfur for the biosyntheses of a variety of cofactors such as biotin, lipoic acid, molybdopterin, and thiamine, as well as Fe-S clusters in proteins and thionucleosides in tRNA (Begley *et al.*, 1999; Marquet, 2001). Although the source has been identified, the biochemical steps for sulfur incorporation into these molecules are poorly understood. Recent studies have provided evidence that always cysteine desulfurases are involved in the initial stages of sulfur trafficking within cells (Mihara *et al.*, 2002).

A major advance in the study of sulfur trafficking has been made by Dean and co-workers. They have found that in *A. vinelandii* the *nifS* gene is part of the nitrogen fixation (*nif*) gene cluster and that the gene deletion has resulted in a mutant unable to produce fully active nitrogenase (Jacobson *et al.*, 1989). Biochemical analysis has revealed that the NifS protein is a homodimeric, pyridoxal 5'-phosphate (PLP)-dependent cysteine desulfurase that catalyzes the conversion of cysteine to alanine and sulfane sulfur via the formation of a protein-bound cysteine persulfide intermediate on a conserved cysteine residue (Fig.9) (Zheng *et al.*, 1993, 1994). This cysteine residue is conserved among all NifS homologs analyzed so far, suggesting that it plays a crucial role. Further analysis of the NifS mechanism revealed the following features: (a) an active site cysteine, Cys₃₂₅, is extremely reactive toward alkylating reagents; (b) the alkylated protein is inactive; (c) substitution of Cys₃₂₅ by alanine eliminates activity; (d) a persulfide could be identified at the Cys₃₂₅ residue position upon incubation of NifS with equimolar amount of L-cysteine substrate (Zheng *et al.*, 1994).

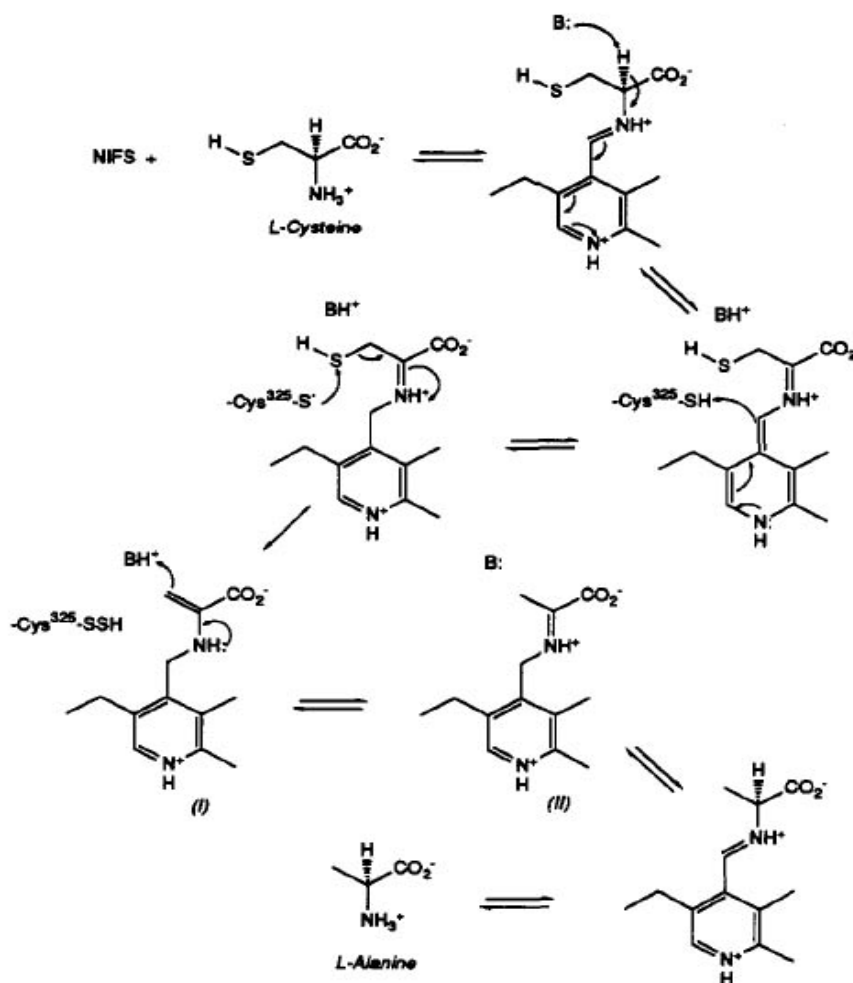


Figure 9: Mechanism of NifS desulfuration reaction

It is now known that NifS-like proteins represent a broad class of proteins that use *L*-cysteine for the general mobilization of S for Fe-S cluster formation, as well as for other sulfur-containing prosthetic groups. Structural and kinetic analyses of several members of this family confirmed and extended the originally proposed mechanism (Leibrecht *et al.*, 1997; Kaiser *et al.*, 2000). On the basis of the biochemical features of NifS, and because it is expressed only under nitrogen-fixing conditions, it turns out that NifS has a role in the specific mobilization of S for maturation of nitrogenase. This possibility was also supported by identification of a *cysE* homolog that is co-transcribed with the *nifS* gene (Evans *et al.*, 1991). The *cysE* gene encodes an O-acetyl serine synthase, which catalyzes the rate-limiting step in cysteine biosynthesis.

In fact, because of the inherent toxicity of free iron and sulfide, the biogenesis of Fe-S clusters is believed to be mediated by specific protein components rather than by spontaneous chemical formation. The key observation relevant to the general process of Fe-S cluster biosynthesis was that inactivation of many *nif* genes results in defects in maturation of either Fe protein or the Fe-Mo protein of nitrogenase enzyme. Deletion of either of two linked genes, *nifU* and *nifS*, uniquely results in substantial loss in activity of both the nitrogenase components (Jacobson *et al.*, 1989). The NifU protein is a cysteine-rich, homodimeric, modular protein with three domains (Agar *et al.*, 2000b; Yuvaniyama *et al.*, 2000). The N-terminal domain has three conserved cysteine residues and binds a labile [2Fe-2S] cluster. The central region contains four conserved cysteine residues and coordinates a stable [2Fe-2S] cluster. The function of the C-terminal domain, which has two conserved cysteine residues, is unknown (Fu *et al.*, 1994; Agar *et al.*, 2000b). All three cysteine residues in the N-terminal domain and all four cysteine residues in the central region of *A. vinelandii* NifU are essential for physiological function (Agar *et al.*, 2000b). NifS and NifU form a weakly bound heterotetrameric complex (Yuvaniyama *et al.*, 2000). Based on these results, it has been proposed that NifU functions as a scaffold for the assembly of a transiently bound Fe-S cluster, from which iron and/or sulfur may be transferred to the apo-form of Fe-S proteins for their maturation.

After the initial demonstration that NifS is a cysteine desulfurase involved in the mobilization of S for nitrogenase maturation, parallel studies were initiated to prove a general role of the cysteine desulfurases in sulfur trafficking. In fact, the ability of *nifS* and *nifU* deletion strains to produce low levels of active nitrogenase and to grow under nitrogen-fixing conditions at an extremely low rate suggested that some other housekeeping function related to generalized [Fe-S] cluster biosynthesis could weakly replace NifU and NifS functions (Jacobson *et al.*, 1989). An homolog of NifS has been identified and named IscS for its proposed role in iron-sulfur cluster biosynthesis (Zheng *et al.*, 1998). IscS and NifS bear a great deal of primary sequence similarity with

a particularly high degree of conservation between their respective active site cysteine and PLP-binding regions. However, the proteins are not functionally equivalent *in vivo* because an *iscS* deletion phenotype cannot be rescued by expression of *nifS* when *A. vinelandii* grows under nitrogen-fixing conditions (Zheng *et al.*, 1998).

A. vinelandii has a paralogous gene to *nifU*, named *iscU*, which is located in a gene cluster composed of *iscR*, *iscS*, *iscU*, *iscA*, *hscB*, *hscA*, and *fdx* (Zheng *et al.*, 1998). Genetic experiments support a key role for the ISC machinery proteins encoded by *iscRSUA-hscBA-fdx* in the assembly of Fe-S clusters, because mutations in the genes decrease the activity of many Fe-S proteins (Schwartz *et al.*, 2000; Skovran *et al.*, 2000; Tokumoto *et al.*, 2001). In addition, over-expression of the gene cluster increases the yield of recombinant Fe-S proteins (Nakamura *et al.*, 1999; Takahashi *et al.*, 1999).

IscU is a homodimeric protein that corresponds to the N-terminal third of NifU (Zheng *et al.*, 1998). Gene knockout studies in bacteria (Tokumoto *et al.*, 2001) have demonstrated a crucial role for IscU in Fe-S cluster biosynthesis. IscU forms a 1:1 complex with IscS (Agar *et al.*, 2000c; Kato *et al.*, 2002), this complex is formed with the C-terminal region of IscS (Urbina *et al.*, 2001). IscU contains three conserved cysteine residues and acts as scaffold for the IscS-directed sequential assembly of $[2\text{Fe-2S}]^{2+}$ and $[4\text{Fe-4S}]^{2+}$ clusters (Agar *et al.*, 2000a, c). These clusters are likely to be inserted into Fe-S apo-proteins in a process that has yet to be fully characterized. Direct transfer of sulfane sulfur from the cysteine persulfide of IscS to the cysteine residues of IscU has been demonstrated: (Smith *et al.*, 2001; Urbina *et al.*, 2001; Kato *et al.*, 2002) covalent complex is formed between IscU and IscS monomers involving a disulfide linkage between Cys₃₂₈ of IscS and Cys₆₃ of IscU. They have also shown that Cys₆₃ of IscU is essential for the IscU-mediated activation of IscS and, based on these results, they proposed that the sulfur transfer from IscS to IscU is initiated by the attack of Cys₆₃ of IscU on the Sy atom of Cys₃₂₈ of IscS that is bound to sulfane sulfur derived from L-cysteine.

1.4 The importance of persulfidic sulfur

Although sulfur is present in many important cofactors, the cellular trafficking for delivering sulfur to these cofactors is still not fully understood (Mueller 2006). Sulfur is a functionally important element of living matter and its chemical flexibility has led to be used in many biomolecules of widely divergent chemical properties that catalyze an impressive range of chemical reactions (Fig 10). Considering the toxicity of the highly reactive bisulfide (HS^-), it turns on that a chemical viable and “safer” sulfur source is necessary for sulfur delivery in the biosynthetic pathways leading to the cofactors and thionucleosides (Kessler 2006).

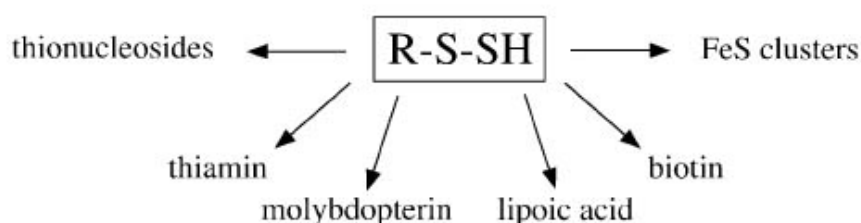


Figure 10: Sulfur compounds relying on persulfidic sulfur (R-S-SH) as sulfur source

In sulfur transfer biochemistry, the role of the chemically versatile persulfide group is emerging (Mueller 2006). The chemistry of persulfide groups is rich because each sulfur can be formally assigned three oxidation states: S^0 (sulfane), S^{-1} (persulfide) or S^{2-} (sulfide). Sulfane sulfur is a potent electrophile (Toohey 1989), susceptible to transfer to a range of nucleophiles, and the more reduced forms of sulfur are nucleophilic. Either sulfur atom in a persulfide group can be nucleophilically attacked to expel the second sulfur as a thiol or bisulfide (S^{2-}), similar to the familiar chemical route of protein disulfide bond exchange. The terminal sulfur of the persulfide group can serve as a nucleophile to form a disulfide bond (R-S-S-R) with an electrophile (Mueller 2006).

Protein persulfide groups are generated by a family of cysteine desulfurases that use the cofactor pyridoxal 5'-phosphate to form a persulfide group on an active site cysteine residue at the expense of the free amino acid cysteine

and generate alanine as the second product (Mihara *et al.*, 2002). The first of these enzymes to be characterized was NifS from *A. vinelandii*, which mobilizes sulfur for the iron-sulfur clusters in the enzyme nitrogenase (Zheng *et al.*, 1994). The terminal sulfur is transferred (formally as S⁰) to cysteine residues in acceptor proteins to make new persulfide groups that are, in turn, used directly in the biosynthesis of a cofactor or thionucleoside or passed to another protein acceptor for the eventual incorporation of sulfur into an end product. The terminal sulfur of the persulfide group on the cysteine desulfurases is handed off to (an)other protein(s) until an enzyme uses the terminal sulfur to synthesize a molecule that the cell needs (Meuller 2006).

The advantage of using persulfidic groups in sulfur trafficking, in addition to its specific chemical properties, is due to the possible molecular interactions especially when the persulfide moiety is carried by a protein. Given the ease of transfer of persulfidic sulfur to thiol acceptors, sulfur relay systems are functional and deliver the active sulfur to specific target sites. Redox reactions of persulfides with thiol–disulfide redox couples are feasible and allow liberation of sulfide when finally required. Persulfides may therefore be regarded as ‘sulfide with a handle’ as with ATP, which presents ‘phosphate with a handle’, a comparison that has already been made by Beinert (2000).

2.Aim

The subjects of the present investigation were *A. vinelandii* RhdA and *E. coli* SseA, that in the rhodanese-domain panorama represent two prototypes of tandem-domain rhodanese proteins. They belong to two different subfamilies: TSTs and MSTs and their active-site motifs, (CRXGX[R/T]) and (CG[S/T]GVT) respectively, are considered important in driving substrate recognition.

In this work, multiple approaches were exploited with the aim of elucidating physiological role(s) of RhdA. We first focused on searching a possible metabolic pathway involving RhdA. Starting from the experimental evidence of direct sulfane sulfur transfer from *E. coli* IscS to RhdA (Forlani *et al.*, 2005), we analyzed whether RhdA could function as sulfane sulfur acceptor of *A. vinelandii* cysteine desulfurases taking in account the importance of the trafficking of the persulfide in the biosynthetic pathways (Meuller 2006).

Secondly, RhdA and SseA biological role(s) were investigated *in vivo*, taking advantage of the availability of an *A. vinelandii* mutant strain lacking *rhdA* gene (Colnaghi *et al.*, 1996) and of an *E. coli* mutant strain lacking *sseA* gene (Celestini 2001). Different growth conditions in presence or in absence of oxidative agents have been evaluated, starting from the evidence that the RhdA null mutant MV474 was more prone than the wild-type strain UW136 to oxidative stress (Cereda *et al.*, 2007).

3.Results

3.1 Details of sulfane sulfur transfer from *E.coli* IscS to RhdA

Starting from the experimental evidence of direct sulfane sulfur transfer from *E. coli* IscS to RhdA (Forlani *et al.*, 2005), the first part of the study was devoted to optimize the time-scale fluorescence assay in order to determine kinetic parameters and some biochemical details of the process.

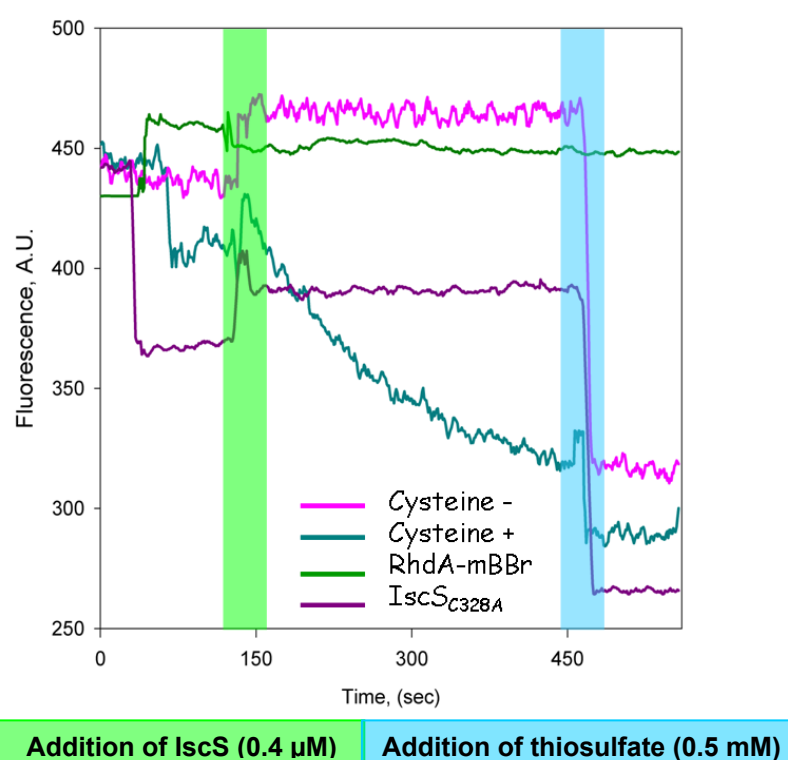


Figure 11: Time-course fluorescence measurements. The intrinsic fluorescence changes ($\lambda_{\text{exc}} = 280 \text{ nm}$, $\lambda_{\text{em}} = 340 \text{ nm}$) were monitored in 1-ml of 50 mM Tris-HCl, 100 mM NaCl (pH 8). The fluorescence traces are: A) pink line, 2 μM sulfane sulfur-deprived RhdA and 0.4 μM IscS in absence of 4 mM *L*-cysteine, B) green line, 2 μM RhdA-mBBr in presence of 4 mM *L*-cysteine and 0.4 μM IscS, C) blue line, 2 μM sulfane sulfur-deprived RhdA in presence of 4 mM *L*-cysteine and 0.4 μM IscS D) violet line, IscS_{C328A} was added to 2 μM sulfane sulfur-deprived RhdA in presence of 4 mM *L*-cysteine.

The potential of this assay to monitoring specific RhdA intrinsic fluorescence changes in a time-scale appropriate to analyze kinetic parameters in various

reaction mixtures was defined using sulfane sulfur deprived RhdA and IscS in presence and in absence of *L*-cysteine, probing sulfane sulfur loading/unloading. As shown in Fig.11, in the presence of *L*-cysteine (blue line), RhdA was able to accept the sulfane sulfur from IscS, thus forming RhdA-SSH as probed by fluorescence decreasing. On the contrary, when the *L*-cysteine was omitted (pink line), the persulfurated form of RhdA was not evidenced because the IscS was not in the persulfurated form. In the absence of IscS and in the presence of *L*-cysteine, no intrinsic fluorescence changes could be detected, thus demonstrating that IscS is the carrier for RhdA persulfuration, (data not shown).

To define the thiols involved in the persulfuration reaction, either a mutant form of *E. coli* IscS (IscS_{C328A}), or an incompetent RhdA form (RhdA-mBBR, where Cys₂₃₀ was chemically blocked) were used. As shown in Fig.11, no RhdA intrinsic fluorescence changes were detected in these situations. These experiments confirmed that the Cys₃₂₈ and the Cys₂₃₀ were the catalytic thiols involved in sulfane sulfur transfer between *E. coli* IscS and RhdA.

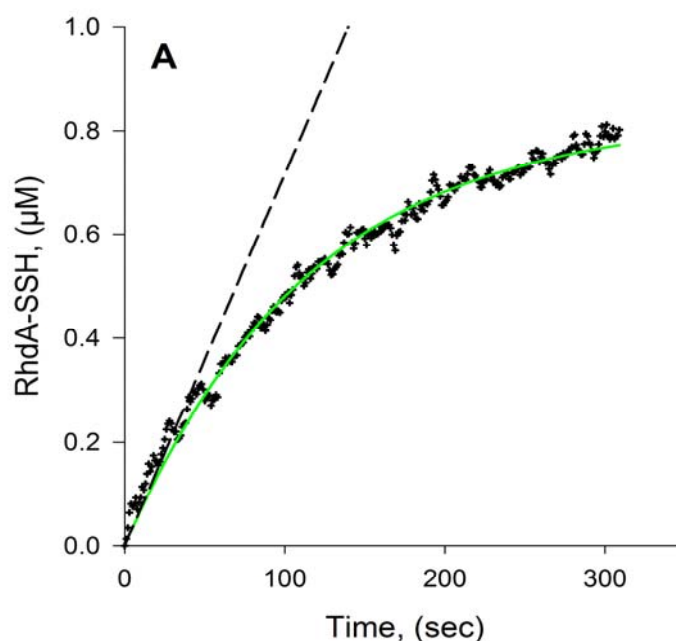


Figure 12: Example of initial rate measurement of IscS-catalyzed RhdA persulfuration.

To calculate the kinetic parameters, the fluorescence data obtained from the persulfuration reaction between IscS and RhdA (first 300 sec) were selected and converted in RhdA-SSH concentration using, as quantitative standard, the fluorescence change value obtained after a complete persulfuration of RhdA (addition of excess thiosulfate). These data were interpolated on a curve (green line, Fig.12) by the following equation:

$$y = a (1 - e^{-bx})$$

The parameters a and b were used to calculate the initial rate (dashed line). Every initial rate, corresponding to a different concentration of RhdA, was calculated and plotted using the double reciprocal plot.

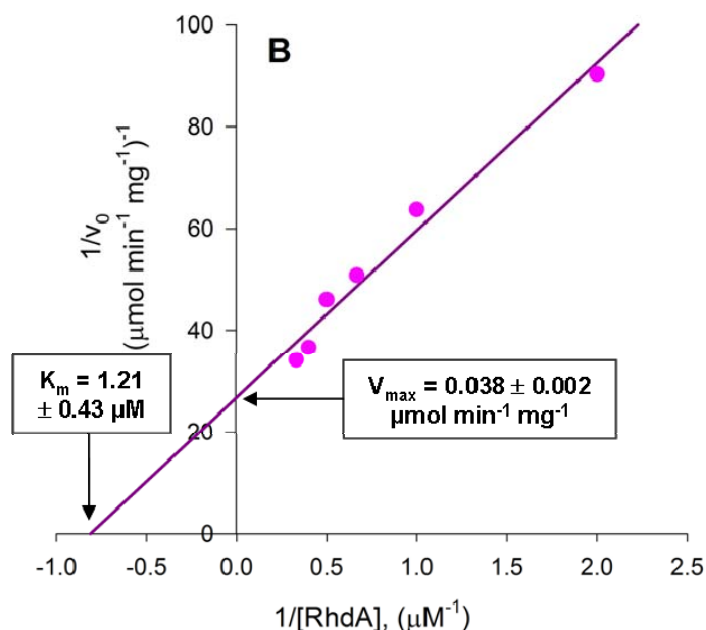


Figure 13: Kinetic analyses of the IscS-catalyzed RhdA persulfuration. Double reciprocal plot analyses, RhdA concentrations were ranged from 0.5 to 3 μM in the presence of 4 mM cysteine. Fluorescence changes were monitored in 1 ml of 50 mM Tris-HCl, 100 mM NaCl (pH 8).

Double reciprocal plot analyses (Fig. 13) indicated that the sulfur transfer exhibits Michaelis-Menten behaviour, suggesting interaction between the persulfide form of IscS and RhdA. The K_m for RhdA persulfuration in this reaction was $1.21 \pm 0.43 \mu\text{M}$, and the turnover number resulted $1.7 \pm 0.09 \text{ min}^{-1}$. The K_m figure for RhdA persulfuration was comparable to that found for cysteine in the desulfuration reaction catalyzed by *E. coli* IscS (Urbina *et al.*, 2001).

The evidence that the *A. vinelandii* RhdA was an acceptor of sulfane sulfur held on the catalytic cysteine residue of *E. coli* IscS, prompted us to investigate whether *A. vinelandii* cysteine desulfurases could promote sulfur transfer to RhdA.

3.2 Expression and purification of *A. vinelandii* cysteine desulfurases

pDB943 and pDB551 were used to over-express IscS and NifS, respectively (Materials and Methods, section 5.2.3). The two protein extracts containing the cysteine desulfurases were applied into a Mono Q 5/50 GL and fractionated using a NaCl gradient (from 0 to 1 M), in presence of 2 mM DTT. NifS was eluted with 0.23 M NaCl and IscS with 0.29 M NaCl. The specific PLP cofactor was used to discriminate the peak of the cysteine desulfurases (absorption at 425 nm). As shown in Fig. 14, the PLP peak (pink line) overlapped that of the cysteine desulfurases (black line).

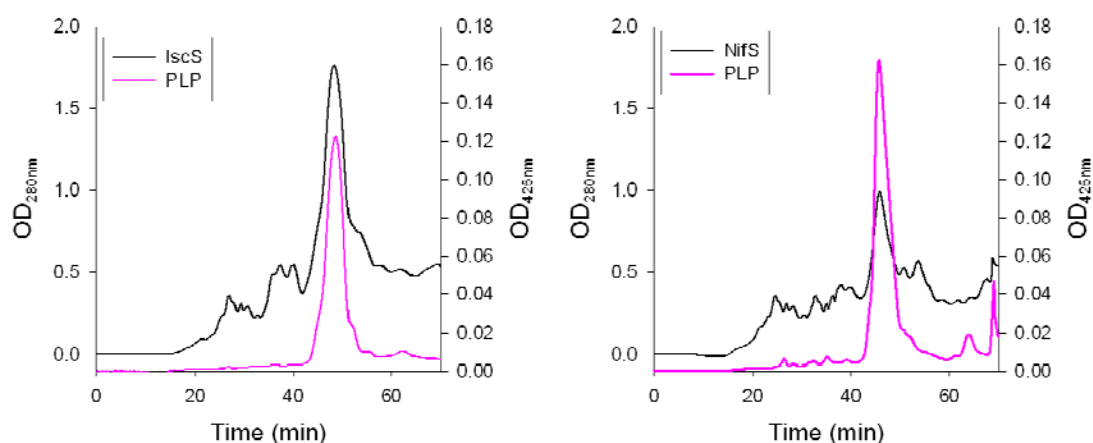


Figure 14: Chromatographic elution profile of the cysteine desulfurases. Samples were applied to Mono Q 5/50 GL and eluted using a NaCl gradient. The proteins were monitored at 280 nm (black line) and at 425 nm (PLP cofactor, pink line).

The purification of the two cysteine desulfurases, starting from the crude extract to the purified protein, was monitored by SDS-PAGE analyses (Fig.15).

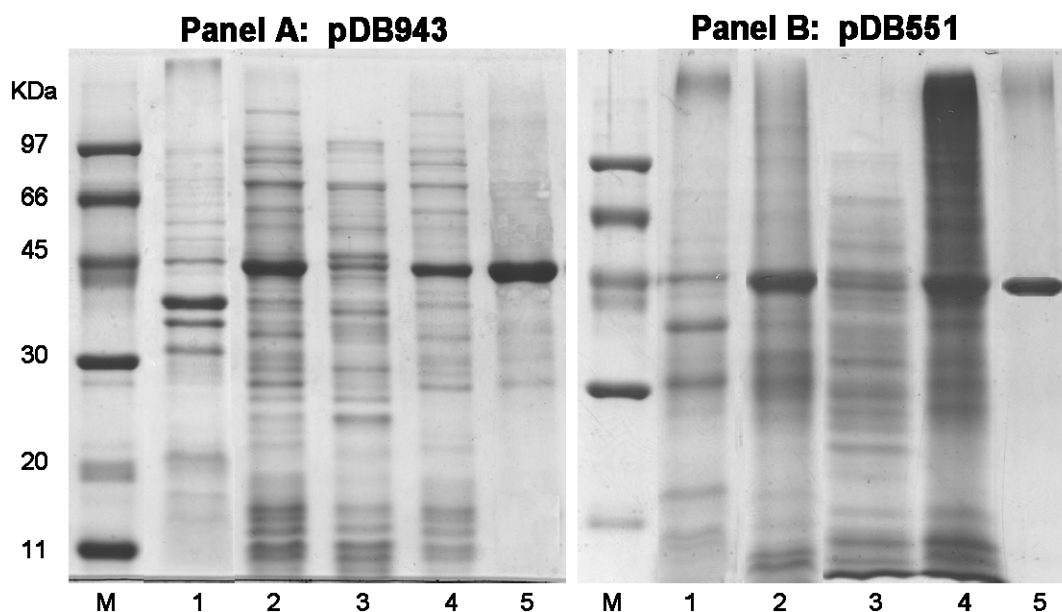


Figure 15: Panel A and B are representative of pDB943 (IscS) and pDB551 (NifS) SDS-PAGE analyses, respectively (under reducing conditions). Marker proteins (size given on the left margin, lane M). Protein extract, insoluble and soluble fraction (lanes 1 and lanes 2, respectively). Ammonium sulphate precipitation supernatants (lanes 3) and pellets after gel-filtration (lanes 4). Purified IscS and NifS after the anionic exchange chromatography (lanes 5).

Panel A and B are representative of pDB943 (IscS) and pDB551 (NifS), respectively. In lanes 2 and in lanes 4 the proteins corresponding to the over-expressed cysteine desulfurase with Mr of 45 KDa are evident. The two cysteine desulfurases obtained after the anionic exchange chromatography are shown in lanes 5, they were used for the experiments described below. Purified IscS was concentrated to 59 μ M and NifS to 37 μ M. During all purification steps, the presence of DTT was necessary to avoid the cysteine desulfurase precipitation.

3.3 Sulfane sulfur transfer between *A. vinelandii* cysteine desulfurases and RhdA

For the aim of validating RhdA–SSH role as sulfur mediator in sulfur transfer processes of physiological relevance, the transpersulfuration process in the presence of the *A. vinelandii* cysteine desulfurases NifS and IscS was studied. Transpersulfuration process defines the direct transfer from the cysteine persulfide of the donor to a thiol of the acceptor protein (Fontecave *et al.*, 2005), therefore we named the reaction here studied as *L*-cysteine:RhdA sulfurtransferase activity.

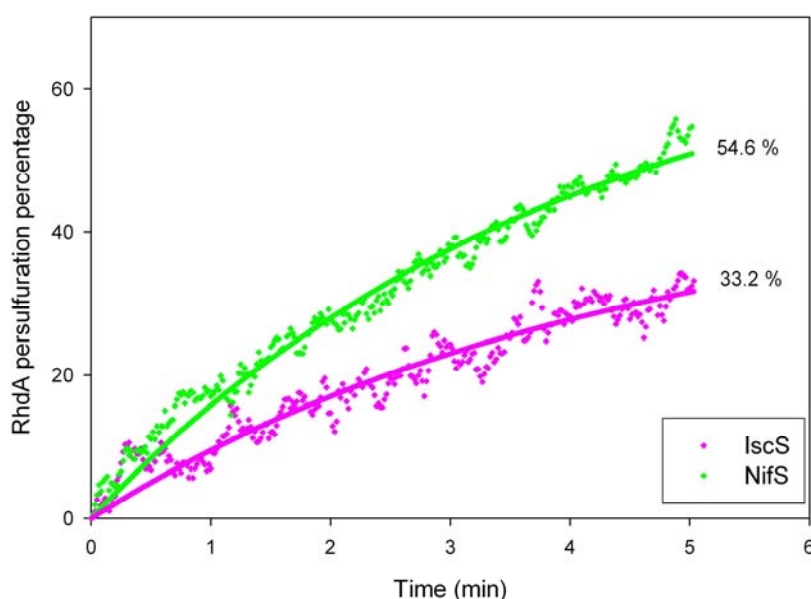


Figure 16: Transpersulfuration of RhdA mediated by cysteine desulfurases in presence of 4 mM cysteine, (time-course fluorescence measurement).

Both *A. vinelandii* cysteine desulfurases were able to generate RhdA-SSH (Fig. 16) and after 5 min reaction, 55% of the RhdA present in the mixture was converted into RhdA-SSH when sulfur was mobilized by NifS, 33% in the case of IscS.

The kinetic parameters of the transpersulfuration reaction (i.e. *L*-cysteine:RhdA sulfurtransferase activity) were determined using the time-

scale fluorescence assay as described in Section 5.4 and the data were analyzed as described in Section 3.1.

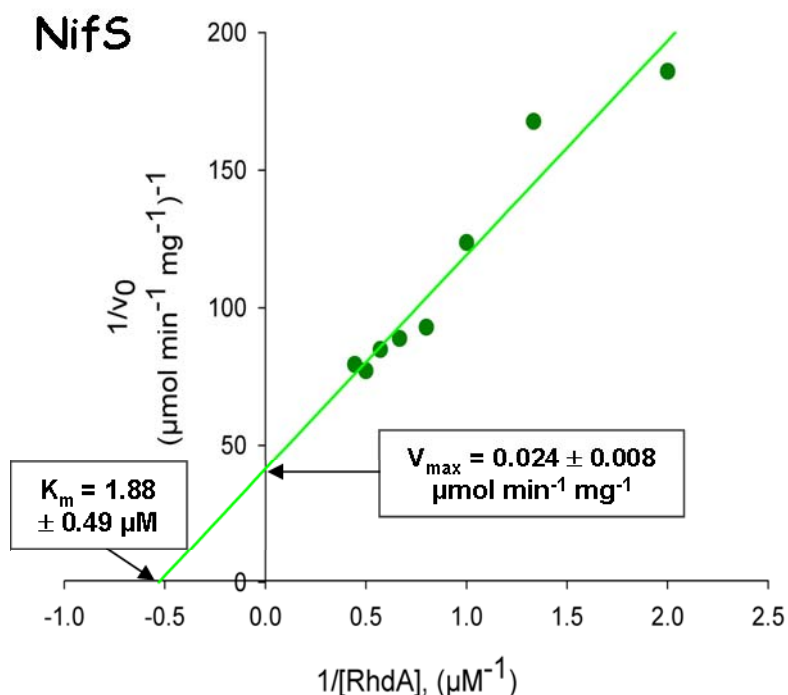


Figure 17: Kinetic analyses of the NifS-catalyzed RhdA persulfuration. Double reciprocal plot analyses, RhdA concentrations were ranged from 0.5 to 3 μM in the presence of 4 mM cysteine. Fluorescence changes were monitored in 1 ml of 50 mM Tris-HCl, 100 mM NaCl (pH 8).

With NifS the sulfur transfer exhibits Michaelis-Menten behaviour (Fig. 17), suggesting interaction between the persulfide form of NifS and RhdA. The NifS kinetic parameters of *L*-cysteine:RhdA sulfurtransferase reaction were: K_m $1.88 \pm 0.49 \mu\text{M}$, and the turnover number $1.05 \pm 0.35 \text{ min}^{-1}$, figures comparable with those found in the presence of *E. coli* IscS (Section 3.1).

As before stated, also *A. vinelandii* IscS showed *L*-cysteine:RhdA sulfurtransferase activity (Fig.16) but, in the concentration range of substrate RhdA used for determining kinetic parameters of NifS-mediated reaction, the data did not yield straight lines in double reciprocal plot analyses (Fig.18). It was reported (Zheng *et al.*, 1998) that kinetic parameters for *A. vinelandii* IscS desulfurization could not be determined because was inhibited by *L*-cysteine concentrations greater than 0.2 mM. This peculiarity could be a

limitation for the production of the persulfurated *A. vinelandii* IscS, the actual sulfur donor to RhdA. Trials to follow the RhdA transpersulfuration reaction in the presence of lower cysteine concentrations did not lead reliable fluorescence changes to quantify RhdA-SSH production.

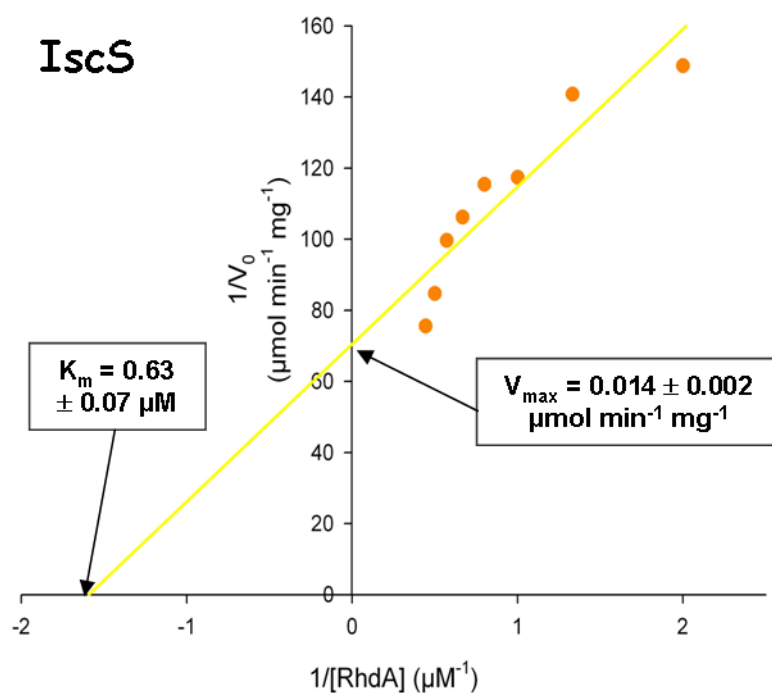


Figure 18: Kinetic analyses of the IscS-catalyzed RhdA persulfuration. Double reciprocal plot analyses, RhdA concentrations were ranged from 0.5 to 2.25 μM in the presence of 4 mM cysteine. Fluorescence changes were monitored in 1 ml of 50 mM Tris-HCl, 100 mM NaCl (pH 8).

3.4 Effects of RhdA on the activity of the *A. vinelandii* cysteine desulfurases NifS and IscS

As above stated, the actual sulfur donor to RhdA was the cysteine desulfurases in their persulfurated form: an intermediate in the *L*-cysteine desulfuration reaction. The results of the RhdA persulfuration efficiency of NifS and IscS (Fig.16) raise the question if the observed sulfur transfer to RhdA reflects the turnover number of cysteine desulfurase activity or structural features between the interacting proteins. To approach this question, either formation of the persulfurated form of both IscS and NifS or their ability to produce alanine were analyzed.

Alanine dehydrogenase assay	
	$\mu\text{mol Ala mg}^{-1}$
NifS	0.51 ± 0.005
NifS + RhdA (1:1)	0.51 ± 0.006
NifS + RhdA (1:2)	0.51 ± 0.008
IscS	0.24 ± 0.002
IscS + RhdA (1:1)	0.28 ± 0.005
IscS + RhdA (1:2)	0.38 ± 0.004

Table 1: Cysteine desulfurase activity measured as production of alanine after 15 min assay, (Material and Methods, section 5.3.3) in the absence and in the presence of RhdA.

The ability of IscS and NifS to produce alanine was different: the NifS activity resulted higher than that of IscS (Table1). In an attempt to investigate whether the transpersulfuration reaction (i.e. the ability of NifS and IscS to transfer sulfane sulfur to RhdA) could favour the cysteine desulfurization, production of alanine was measured in the presence of RhdA. As shown in Table 1, RhdA did not affect the activity of NifS but it seems to affect the activity of IscS. In the presence of equimolar amount of RhdA/IscS, the

increase of IscS activity was less pronounced (increase of 17%) than it was in the presence of RhdA at molar ratio IscS/RhdA of 1/2 (increase of 58%).

Sulfane sulfur assay	
	$\mu\text{mol CNS}^- \text{mg}^{-1}$
NifS	0.036 ± 0.002
NifS + RhdA	0.068 ± 0.006
IscS	0.104 ± 0.008
IscS + RhdA	0.139 ± 0.009
RhdA alone	0.01 ± 0.0001

Table 2: Sulfane sulfur released from the cysteine desulfurases after 15 min assay (Material and Methods, section 5.3.2) in the absence and in the presence of RhdA, (molar ratio 1:2 cysteine desulfurase/RhdA).

Sulfane sulfur detection as ferric-thiocyanate complex (Materials and Methods, section 5.3.2) was used to quantify the formation of NifS-SSH and IscS-SSH (Table 2). Formation of IscS-SSH was higher than that of NifS-SSH. The sulfane sulfur assay was carried out also in the presence of RhdA and, as shown in Table 2, we found an increase of the persulfuration of both cysteine desulfurases.

The two methods used to determine the cysteine desulfurases activity (i.e. production of alanine and of the persulfurated form of the enzyme) did not show the same trend. It resulted that, IscS-SSH formation was higher than NifS-SSH formation, although this latter cysteine desulfurase was more active in producing alanine than it was IscS. These puzzling results might be explained by considering that in the alanine dehydrogenase assay, DTT was necessary to release the sulfur from the cysteine desulfurases. Differently, when the persulfurated form of the cysteine desulfurases was measured as ferric-thiocyanate complex, the nucleophilic cyanide was the sulfur acceptor. The different behaviors of the cysteine desulfurases in the measurements was probably due to the presence of the DTT. The “DTT effect” was underlined when the assays were carried out in the presence of RhdA. In the

case of alanine dehydrogenase assay the presence of RhdA did not significantly modulate the cysteine desulfurase activity. In the case of RhdA-SSH, we previously found that DTT was less effective in sulfur release from RhdA as compared to cyanide, (46 U/mg compared to 900 U/mg), (Forlani *et al.*, 2003), a feature that could explain the different results obtained in the two assays.

3.5 Searching protein-protein interactions

Transpersulfuration reactions likely imply interaction between sulfur donor and acceptor protein. To investigate whether a complex between cysteine desulfurases and RhdA could be formed, we at first carried out size-exclusion chromatography experiments (Yang *et al.*, 2006).

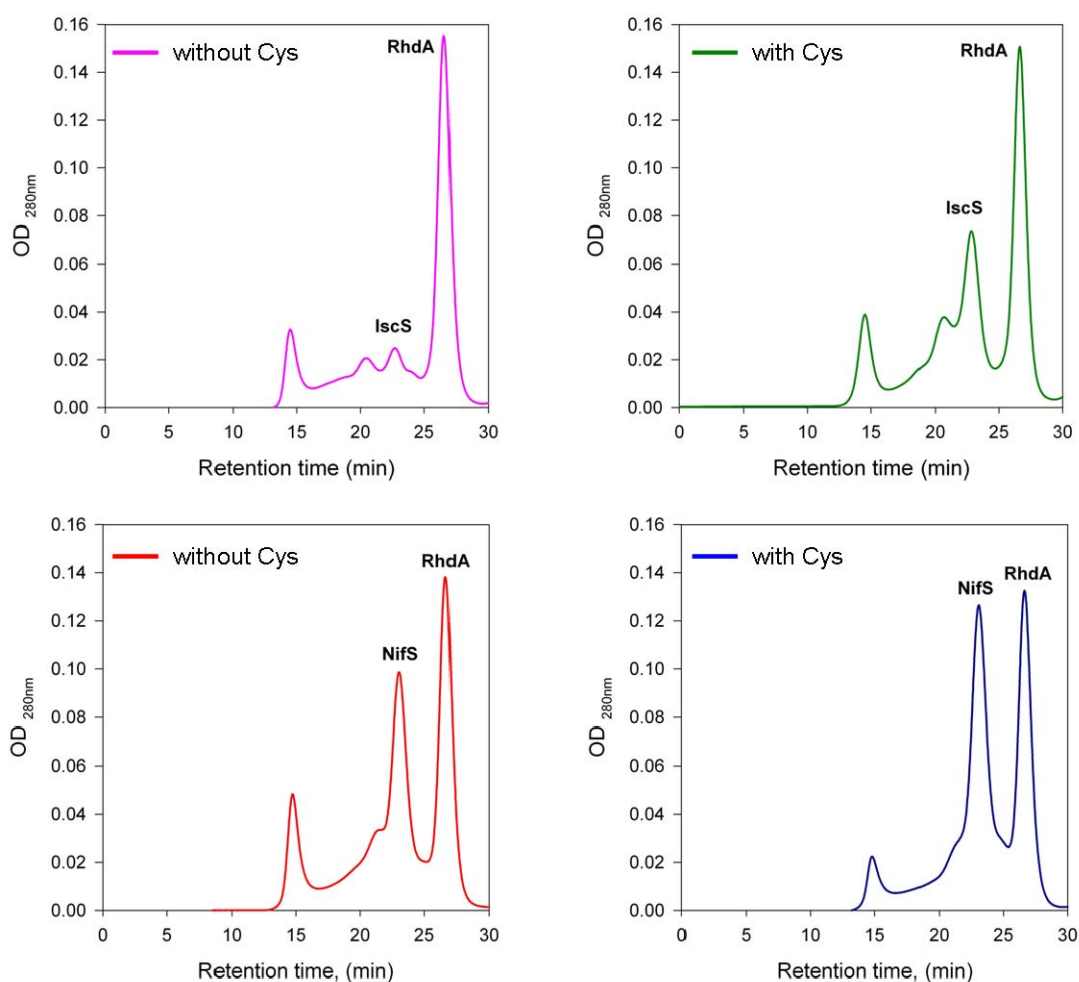


Figure 19: Size-exclusion chromatography experiments (Superose 12, see Materials and Methods). The chromatograms obtained after incubation (1 h) of the cysteine desulfurases and RhdA, in the absence and in the presence of 4 mM Cys.

As shown by fluorimetric assays, cysteine was mandatory for the transpersulfuration reaction and an hypothetical complex between RhdA and the cysteine desulfurase was pictured. The cysteine desulfurases from *A.*

vinelandii were incubated with RhdA in the presence and in the absence of cysteine, (Materials and Methods, section 5.5.1). As shown in Fig.19, the presence of cysteine cause changes in the elution profile either with IscS or NifS. The “cysteine effect” should be due to the fact that cysteine acts as reducing agent on the cysteine desulfurase aggregates promoting the formation of the homodimeric form. Unfortunately, in the presence or in the absence of cysteine, SDS-PAGE analyses did not reveal the formation of any complex between the cysteine desulfurases and RhdA, (data not shown).

To better study possible protein-protein interactions between RhdA and the cysteine desulfurases, immunochemical approaches were exploited.

Affi-Gel Hz affinity chromatography was used at first, (Materials and Methods, section 5.5.2) and as shown in Fig.20, the majority of UW136 proteins were unbound.

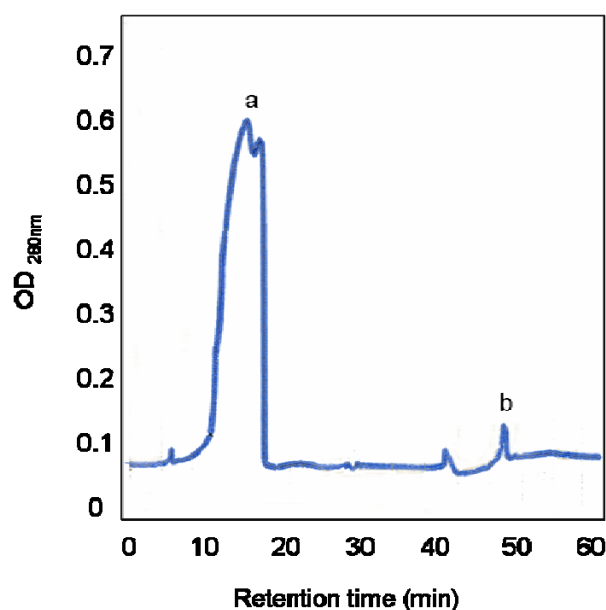


Figure 20: Chromatogram obtained from the affinity chromatography Affi-Gel Hz (Materials and Methods, section 5.2.1). a) peak of UW136 unbound proteins; b) peak of UW136 proteins bound to the anti-RhdA antibodies.

In Fig.21, lane 3 represent the protein bound to the anti-RhdA antibodies fixed at the Affi-Gel. Unfortunately, the antibodies were co-eluted with the

antigen and the hypothetical interacting proteins. It was impossible visualize them on SDS-PAGE also because the amount of protein bound to the antibodies was too scarce.

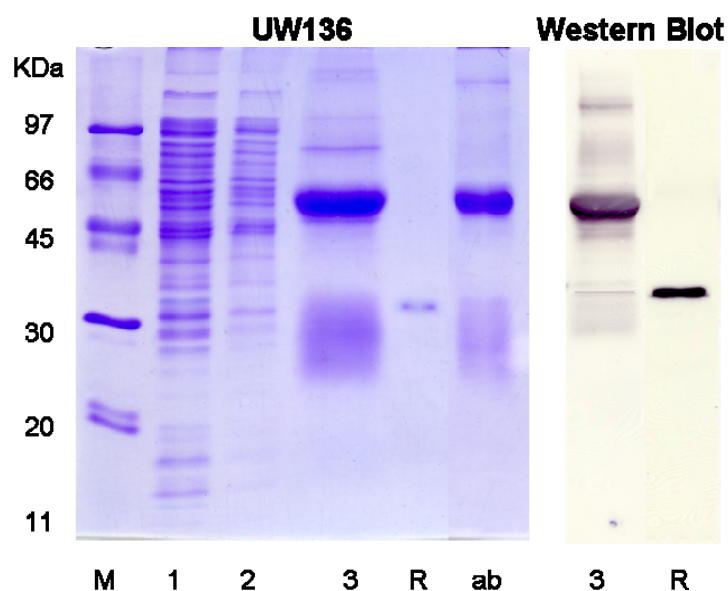


Figure 21: SDS-PAGE analyses of immunoaffinity chromatography (under reducing conditions). Lane M denotes marker proteins, (size given on the left margin); lane 1 represents the protein extract, lane 2 the unbound proteins and lane 3 the bound proteins. Lane R represents purified RhdA and lane ab represents purified anti-RhdA antibodies. On the right side Western Blot was shown.

To overcome troubles likely derived from the instability of anti-RhdA antibodies to the acidic treatment necessary in the above immunochemical approach, we used CNBr activated Sepharose 4B. Also in this case, the proteins eluted, (RhdA and some interacting proteins), were in too scarce amount to be visualized by SDS-PAGE (data not shown).

To enhance the sensibility of the method, we exploited an immunoaffinity chromatography by using HiTrap Protein A HP (see Materials and Methods, section 5.5.2). The elution profile obtained from the HiTrap Protein A HP (Fig.22) was similar to the two obtained with the previously columns. Also in this case, we were not able to detect any complex (SDS-PAGE analyses not shown). At the moment, we are therefore not able to define whether a complex between RhdA and some other interacting proteins could be formed:

probably the interactions were too weak to produce a stable detectable complex.

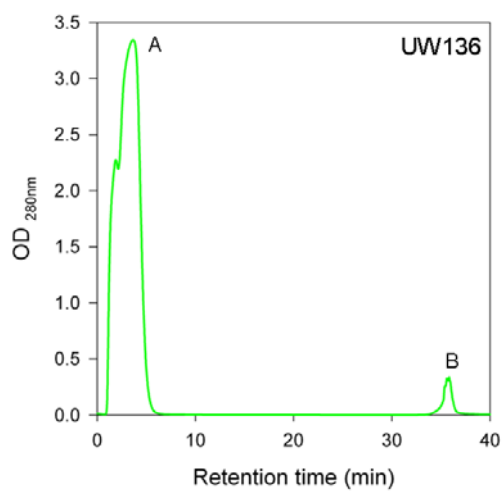


Figure 22: HPLC chromatogram obtained from HiTrap Protein A HP chromatography. A) represents the unbound protein from UW136 extract, (Materials end Methods, section 5.2.1); B) represents mixture of the anti-RhdA antibodies and the UW136 bound proteins.

3.6 Phenotypic difference between *E.coli* Δ sseA6 and *A. vinelandii* Δ rhda

The active-site motifs CRXGX[R/T] and CG[S/T]GVT (where square brackets indicate alternative residues, 'X' any amino acid) are usually found in TSTs and in MSTs, respectively (Nagahara *et al.*, 1995-1996; Papenbrock *et al.*, 2000; Colnaghi *et al.*, 2001). The active-site loop of known TSTs always contains two basic residues (i.e. if the last loop residue is Thr, a basic residue is observed at one of the X positions), whereas no charged residues are observed in biochemically characterized MSTs. These structural features might be related to the distinct ionic charge of the respective *in vitro* substrates, thiosulfate (2⁻) for TSTs and 3-mercaptopyruvate (1⁻) for MSTs. Such differences may provide the structural bases for the specific catalytic mechanisms which distinguish TSTs from MSTs.

RhdA and SseA are representative prototypes of tandem-domain rhodanese proteins (Bordo *et al.*, 2000; Spallarossa *et al.*, 2004), belonging to two different subfamilies: TSTs and MSTs, respectively. *E. coli* SseA represents a prototype of bacterial tandem domain rhodanese proteins displaying MST in agreement with its active site motif (CGSGVT) (Spallarossa *et al.*, 2004). The tandem rhodanese domain *A. vinelandii* RhdA *in vitro* displays TST activity and its active site motif (HCQTHHR) is not commonly shared by other bacterial TSTs (Colnaghi *et al.*, 1996; Bordo *et al.*, 2001; Pagani *et al.*, 2000). Considering that specific active site motif could infer different biological functions of the widespread rhodanese-like proteins, we undertook an investigation to define some phenotypic features of the *A. vinelandii* mutant MV474, lacking the *rhda* gene and of the *E. coli* mutant Δ sseA6, lacking the *sseA* gene.

3.6.1 Effects of *rhdA* deletion on *A. vinelandii* growth

To establish the effects of *rhdA* deletion on *A. vinelandii* growth, the wild type UW136 and the *rhdA* mutant MV474 strains were grown up in the presence of ammonium acetate (i.e. BSN) and in diazotrophic conditions (i.e. in the absence of ammonium acetate, BS).

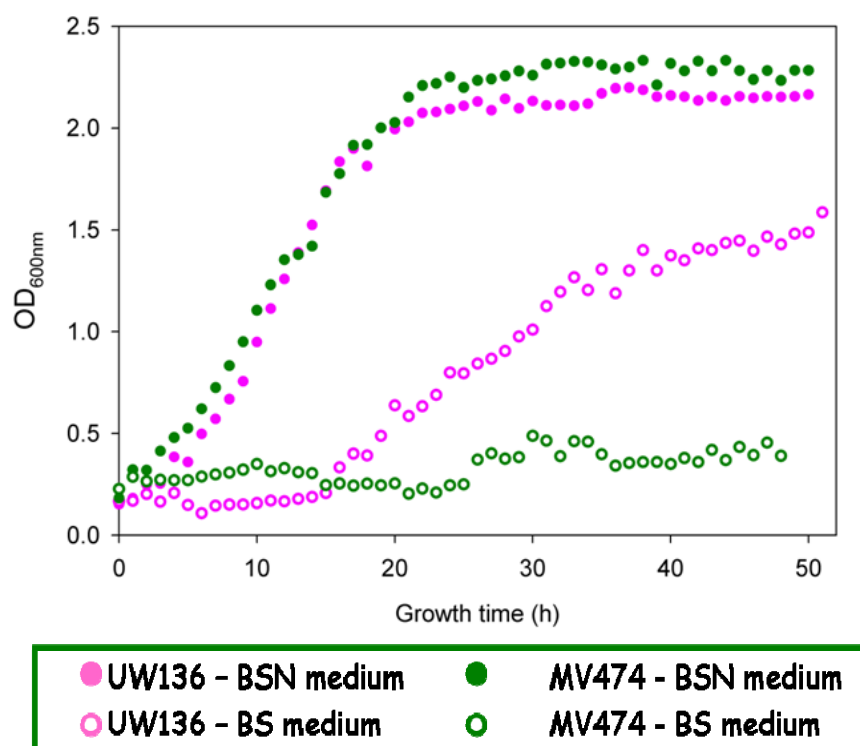


Figure 23: *A. vinelandii* growth curves. UW136, the wild-type strain, and MV474, *rhdA* null mutant, were grown in Burk's medium supplemented with sucrose and in the presence (BSN) or in the absence (BS) of ammonium acetate, (Materials and Methods, section 5.1).

As shown in Fig. 23, UW136 and MV474 did not show any difference in growth when ammonium acetate was present. On the contrary, in diazotrophic conditions, UW136 and MV474 showed a long lag phase with respect to the growing in BSN. Moreover, MV474 showed impairment in growing as compared to the wild type strain when growth up was in BS conditions. Apparently the deletion of *rhdA* gene could be related to nitrogen fixation, inducing the block of the MV474 growth. Moreover, we must take in account that *nifS* gene is involved in the nitrogen fixation metabolisms and mostly expressed under diazotrophic condition (Jacobson *et al.* 1989).

Moreover, in BSN conditions, it was found (Cereda *et al.*, 2007) that the RhdA null mutant MV474 was more prone than the wild-type strain UW136 to oxidative stress. In the absence of RhdA the resistance in condition mimicking oxidative stress (i.e. the addition of the oxidative agent PMS) was significantly impaired. In the case of RhdA mutant, the OD_{600nm} recorded after 16 hours PMS treatment was about 40% of that of untreated control cultures, whereas comparable OD_{600nm} was recorded for the wild type strain, no matter PMS exposure. These results indicated that the two domain rhodanese RhdA could trigger protection for oxidative events in *A. vinelandii*.

3.6.2 Effects of *sseA* deletion on *E. coli* growth

In an attempt to investigate whether the absence of the two domain rhodanese-like protein SseA could infer specific phenotypic features to *E. coli*, growth profiles of *E. coli* wild type strain and $\Delta sseA6$ mutant strain were compared by exploiting different growth media and carbon sources (Fig.24).

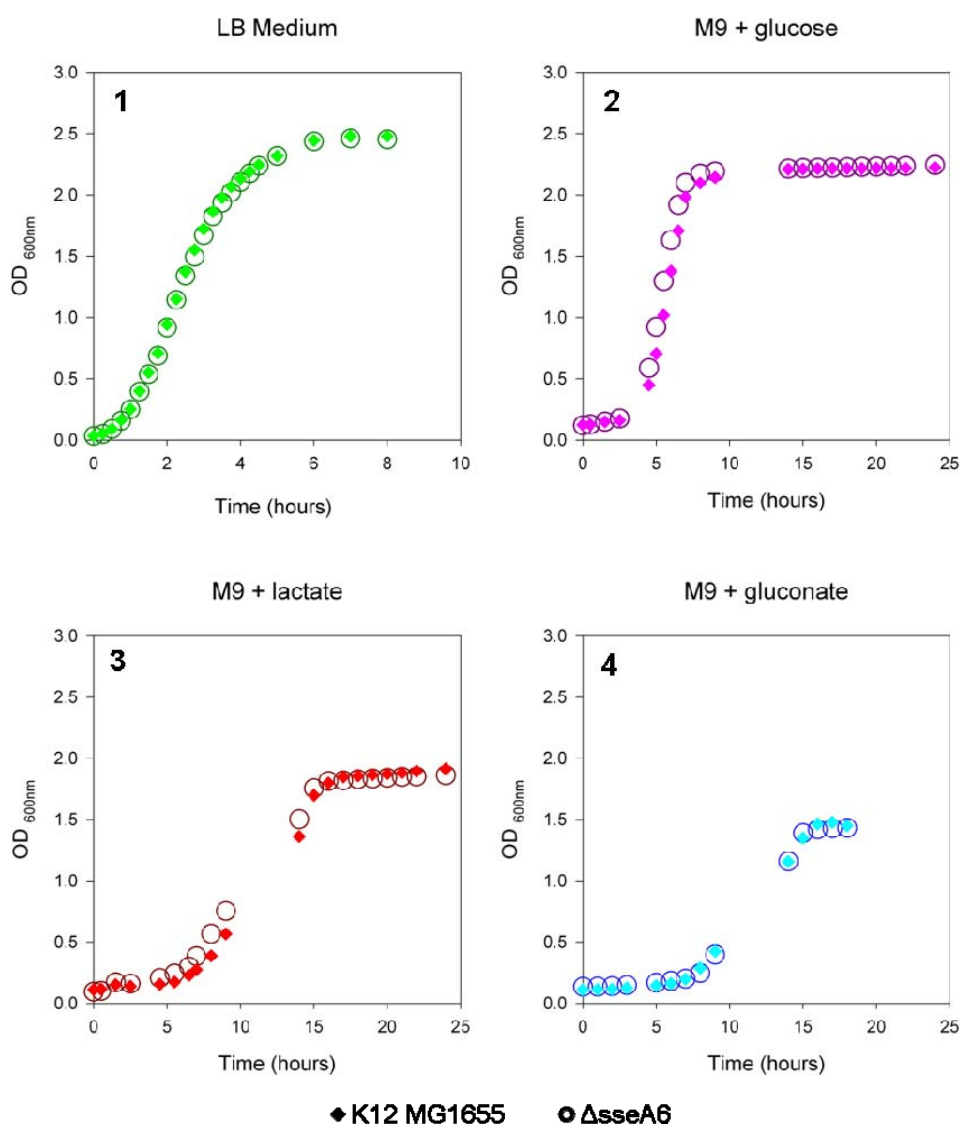


Figure 24: *E. coli* growth curves. K12 MG1655, the wild-type strain, and $\Delta sseA6$, *sseA* null mutant, were grown aerobically in different culture medium at 37 °C. In panel 1 was represented the growth in Luria Bertani Broth and in panel 2, 3 and 4 the growth in M9 minimal medium with different carbon source, (Material and Methods, section 5.1).

Panel 1 shows the growth curves of the wild type strain K12 MG1655 and of the mutant $\Delta sseA6$ strain in the complete medium Luria Bertani Broth (Material and Methods, section 5.1). Panel 2, 3 and 4 show the *E. coli* wild type and the mutant strains growth curves using the minimal medium M9 in the presence of different carbon sources, (i.e. glucose, lactate and gluconate). In all the media tested, the deletion of *sseA* gene did not impaired growth of *E. coli*, since overlapped growth curves (wild type vs mutant strain) were found.

3.6.3 Effects of *sseA* deletion on *E. coli* growth in conditions mimicking oxidative stress

To investigate whether SseA, as it was for RhdA, could protect *E. coli* from oxidative events, *E. coli* growth was analyzed in condition mimicking oxidative stress, by addition of either phenazine methosulfate (PMS) (Nachin *et al.*, 2003) or hydrogen peroxide (Antelmann *et al.*, 1996). The cells were grown up to reach the exponential phase, then the cultures of either K12 MG1655 and $\Delta sseA6$ strains were divided into two equal samples, one of which was treated with the oxidative agent.

The results of the PMS investigation are shown in Fig.25. Panel 1 shows the growth curves of K12 MG1655 and $\Delta sseA6$ in LB Broth; panel 2, 3 and 4 show the growth curves of the two *E. coli* strains in minimal medium M9 in presence of different carbon sources (i.e. glucose, lactate or gluconate). In all conditions tested, wild type and mutant strain growth profiles were overlapped. As shown in panel 1 and 2, after the addition of 25 μM PMS, both strains did not stop growing. In panel 3, two cases are represented: when PMS was 15 μM , both strains were not influenced by the oxidative agent, on the contrary, at PMS 25 μM , both strains stopped growing. In panel 4 is shown that the addition of 15 μM PMS severely affected the growth of both strains when gluconate was the carbon source used.

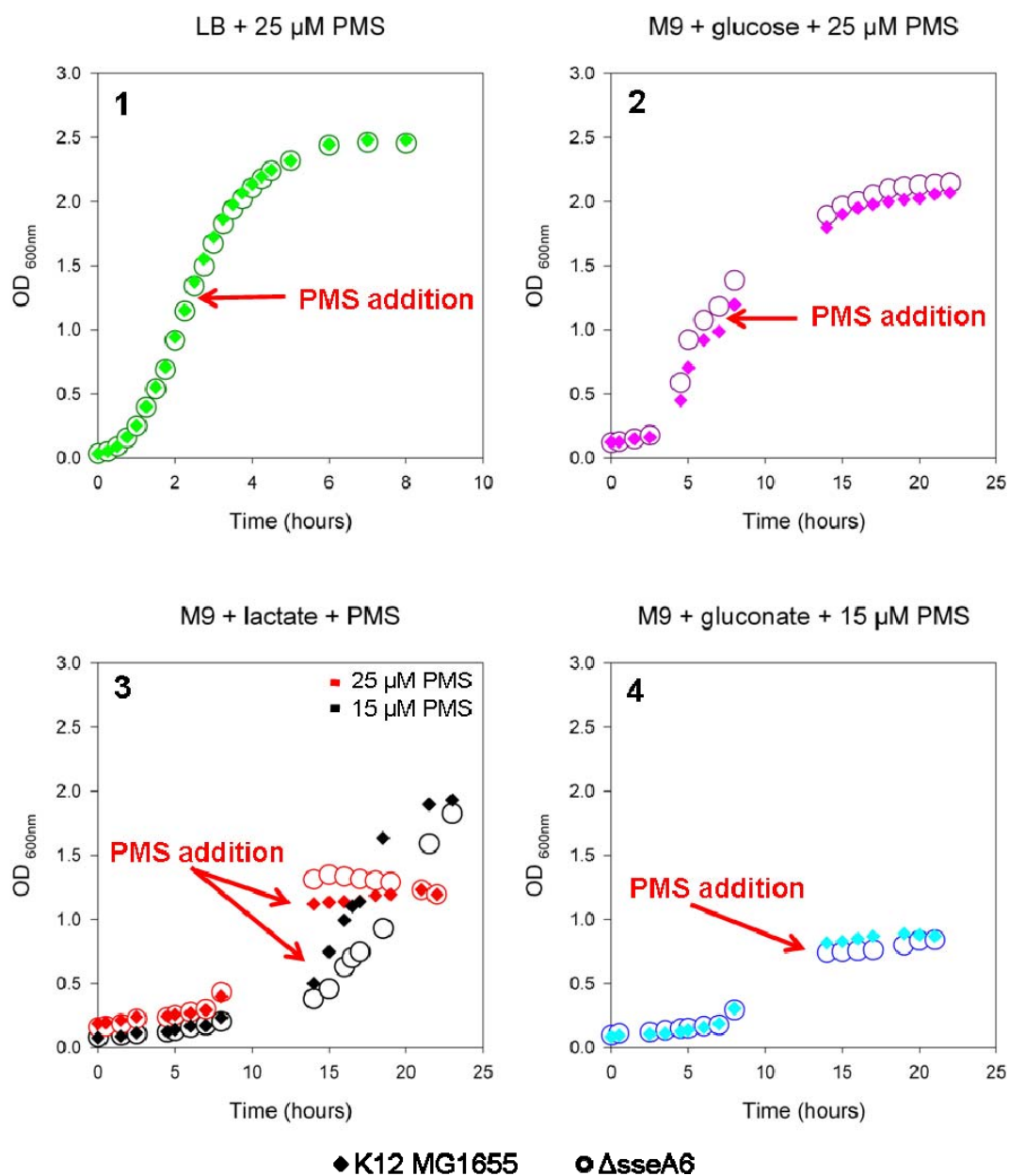


Figure 25: *E. coli* growth curves. *K12 MG1655*, the wild-type strain, and *ΔsseA6*, *sseA* null mutant, were grown aerobically in different culture medium at 37 °C. In panel 1 was represented the growth in Luria Bertani Broth and in panel 2, 3 and 4 the growth in M9 minimal medium with different carbon source, (Material and Methods, section 5.1). 15 or 25 μM PMS was added as oxidative agent during the exponential phase.

The differences in growing were due to the different carbon sources used. In fact, glucose and lactate must enter in the glycolysis pathway, on the contrary, gluconate is the first intermediate of the Entner-Doudoroff pathway (Peekhaus *et al.* 1998). Catabolism of gluconate via the ED pathway in *E.*

coli is controlled by the GntR regulon, that is subject to cyclic AMP (cAMP)-dependent catabolite repression (Egan *et al.*, 1992, Porco *et al.* 1997, Tong *et al.* 1996). Gluconate interacts either as inducer or as repressor with adenylate cyclase. In the presence of cAMP, the growth on gluconate results in accumulation of methylglyoxal that inhibit the bacterial growing (Bächi *et al.* 1975) and an intracellular accumulation of 2-keto-3-deoxy-6-phosphogluconate (KDPG), the key intermediate of ED pathway, that is bacteriostatic (Fuhrman *et al.* 1998).

The results of growing experiments are summarized in Fig.26. The two *E.coli* strains grown in different medium and treated or untreated with PMS did not evidence any significant difference.

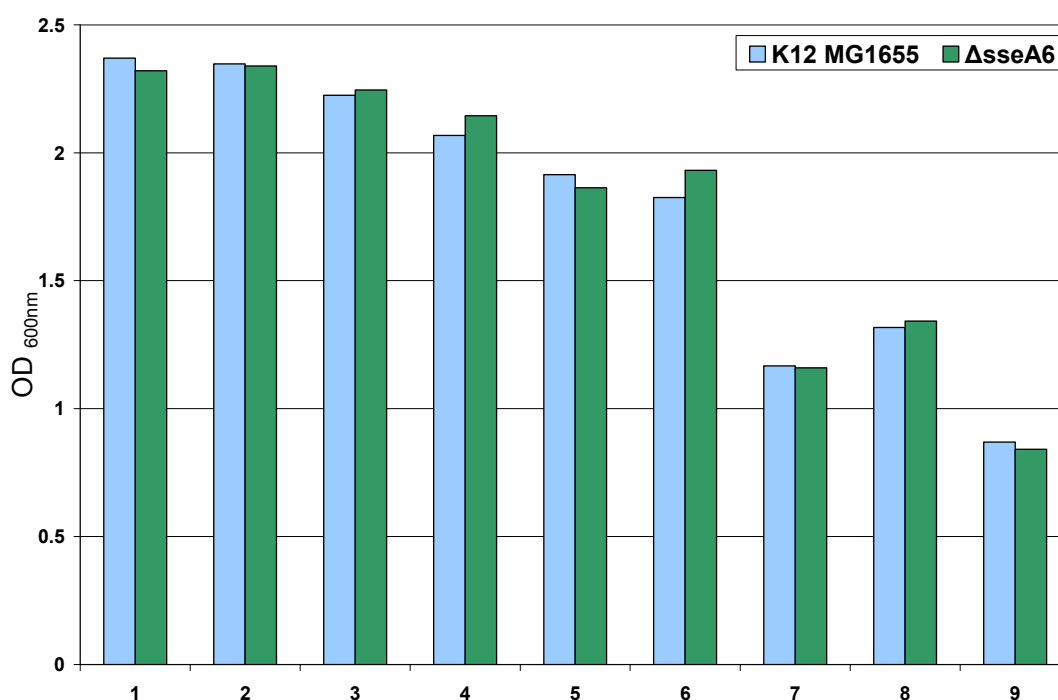


Figure 26: Effect of phenazine methosulfate (PMS) on growth of *E. coli* wild type (K12 MG1655) and *sseA* mutant (Δ sseA6) strains. Growth of K12 MG1655 and Δ sseA6 strains in different medium was estimated by measuring the OD_{600nm}. 1 and 2 represent the growth of both strains in LB Broth without and with 25 μ M PMS, respectively; 3 and 4 represent the growth of both strains in M9 minimal medium with glucose (as carbon source) without and with 25 μ M PMS, respectively; 5, 6 and 7 represent the growth of both strains in M9 minimal medium with lactate (as carbon source) without and with 15/25 μ M PMS, respectively; 8 and 9 represent the growth of both strains in M9 minimal medium with gluconate (as carbon source) without and with 15 μ M PMS, respectively.

To wide investigate the response of the *sseA* mutant and the wild type strains to oxidative stress conditions, the effect of hydrogen peroxide was analyzed.

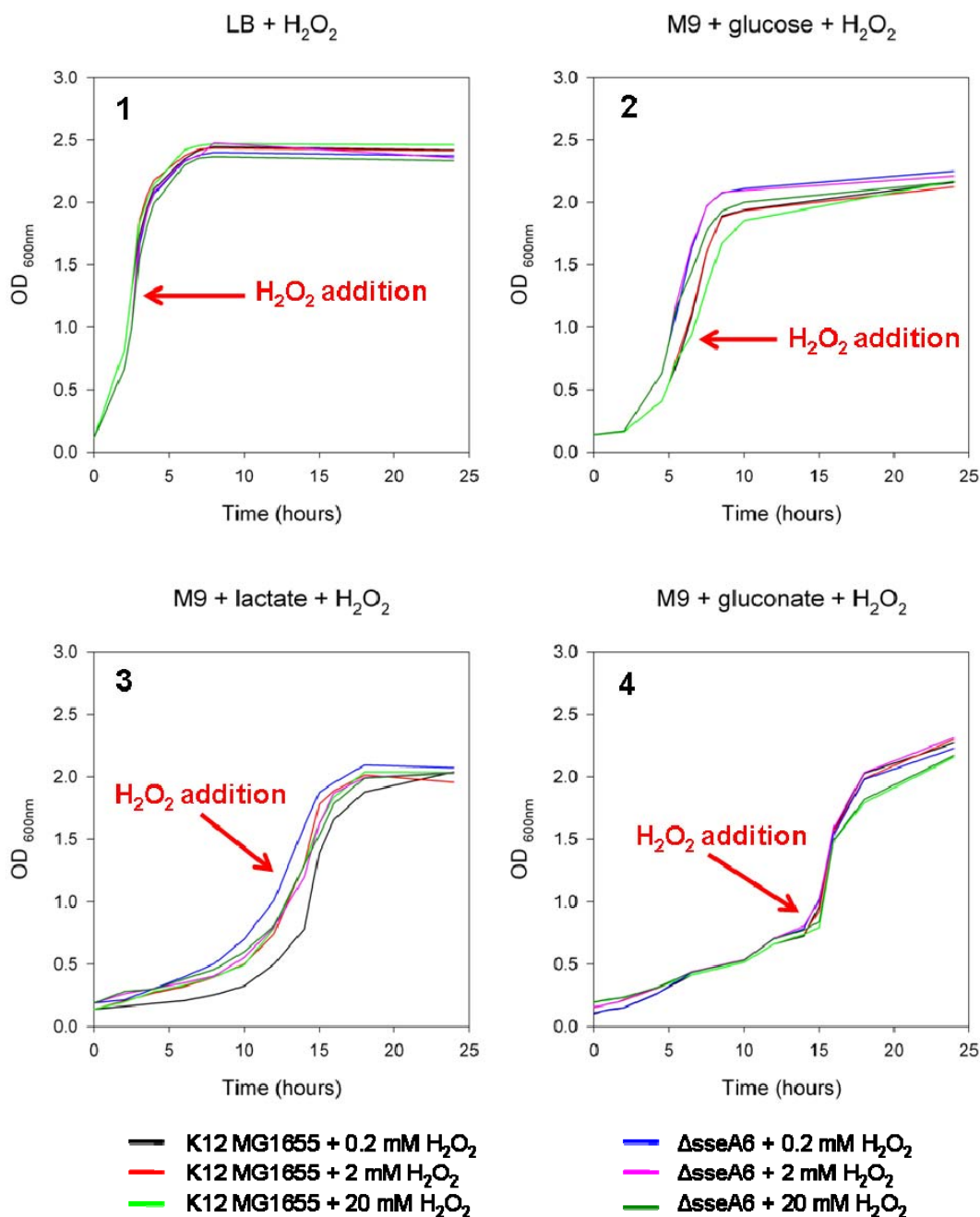


Figure 27: *E. coli* growth curves. K12 MG1655, the wild-type strain, and Δ sseA6, *sseA* null mutant, were grown aerobically in different culture medium at 37 °C. In panel 1 was represented the growth in Luria Bertani Broth and in panel 2, 3 and 4 the growth in M9 minimal medium with different carbon source, (Material and Methods, section 5.1). 0.2, 2 or 20 mM H₂O₂ was added as oxidative agent during the exponential phase.

The results of the H₂O₂ investigation are shown in Fig.27. Panel 1 shows the growth curves of K12 MG1655 and Δ seA6 in LB Broth; panel 2, 3 and 4 show the growth curves of the two *E. coli* strains in minimal medium M9 in presence of different carbon sources (i.e. glucose, lactate or gluconate). The growth curves of wild type and mutant strains are overlapped. Also increasing amount of H₂O₂ (ranging from 0.2 to 20 mM) did not underline any difference in growth between the wild type and the mutant strains.

4. Concluding remarks

In the sulfur incorporation system that rely on persulfide chemistry, involvement of rhodanese homology domain proteins is emerging. It was, indeed, shown that the catalytically essential Cys₄₅₆ in the rhodanese homology domain of ThiI was a recipient of the terminal sulfur of the persulfide form of IscS in the biosynthesis of 4-thiouridine in tRNA (Palenchar *et al.* 2000), and that the rhodanese homology domain of the human enzyme MOCS3 transiently bears a persulfide group on the pathway of sulfur incorporation into molybdopterin (Matthies *et al.* 2004 – 2005). In *A. vinelandii* rhodanese RhdA (Colnaghi *et al.* 1996), the catalytic loop structure and electrostatics (Bordo *et al.* 2000 - 2001; Pagani *et al.* 2000) appear properly designed to support stabilization of a persulfide bond on its Cys₂₃₀ catalytic residue. In *E. coli*, however, recombinant RhdA is expressed either in the persulfurated form or in the sulfane sulfur-deprived form, depending on the sulfur source present during the growth. We found that *L*-cysteine was the effective sulfur source of RhdA persulfuration, and that the cysteine desulfurase IscS present in *E. coli* promoted the production of RhdA in the persulfurated form (Forlani *et al.* 2005). Considering the peculiarity of RhdA active site in favoring the stabilization of its persulfurated form, it became conceivable that RhdA-SSH could function as “escort” protein(s) during sulfur mobilization processes. In order to frame RhdA-SSH functions in a cellular context, we first investigated whether direct transfer of S⁰ from the IscS-like enzymes of *A. vinelandii* occurred. In the present study evidences of different modality of interactions of RhdA with *A. vinelandii* NifS and IscS are provided. Both *A. vinelandii* cysteine desulfurases were able to generate RhdA-SSH but only NifS exhibits Michaelis-Menten behaviour. *nifS* gene is involved in the nitrogen fixation metabolisms and mostly expressed under diazotrophic condition (Jacobson *et al.* 1989). Studies on *rhda* deletion effects on *A. vinelandii* strains, (wild type UW136 and *rhda* mutant MV474), grown under diazotrophic conditions, shown an impairment in growing between the two strains, apparently connecting the deletion of *rhda* gene and the nitrogen fixation.

The results of the present study make RhdA an acceptor of the sulfur mobilized by the *A. vinelandii* cysteine desulfurases and evidence has been

provided that interaction with RhdA increased persulfide formation on IscS. Activation of *E. coli* cysteine desulfurase IscS by interacting partners was observed (Kambampati *et al.* 1999; Kato *et al.* 2002; Ikeuchi *et al.* 2006), and the findings that the activity of IscS was regulated by partner proteins led to the proposal that, by changing binding partners, IscS selects the sulfur flow through various sulfur trafficking pathways in the cell (Ikeuchi *et al.* 2006). Unfortunately, the failure in demonstrating specific molecular interactions between RhdA and the *A. vinelandii* cysteine desulfurases, an event that could address investigations on cellular pathways in which RhdA could be used as sulfur-delivering protein to a possible target, did not allow us to define physiological routes of the persulfidic form of RhdA.

In attempt to elucidating relationships between active-site structural motives and interactions in rhodanese-domain proteins, we studied the “model *Escherichia coli*” which is the prototype of organism containing all rhodanese-domains architectures (up to 9) unless rhodanases with catalytic loop of *A. vinelandii* RhdA.

In particular, the *E. coli* *sseA* gene encodes for tandem rhodanese domain protein SseA, previously characterized in our lab (Colnaghi *et al.* 2001; Spallarossa *et al.* 2004) that is endowed with 3-mercaptopyruvate-dependent sulfurtransferase activity (MST). In the present study, analyses of the growth behaviors of the *E. coli* Δ *sseA6*, as compared to the incoming evidence of a role of RhdA in protecting *A. vinelandii* from oxidative events leading to the inactivation of vulnerable Fe-S proteins (Cereda *et al.* 2007), indicated that the metabolic networks “targets” of these prototypes of tandem domain rhodanese proteins are different. No one, however, of the growing conditions where the lack of RhdA inferred growing deficiency of *A. vinelandii*, was found alter growth of *E. coli* Δ *sseA6*, as compared to the wild-type strain. These results enhance the idea that structural features (e.g. active site motif) of the widespread rhodanese-like proteins make them functional devices in different metabolic context.

5.Materials and methods

5.1 Strains, media and bacterial cultures

The bacterial strains used are listed in the following table:

Bacterial species	Strain	Genotype	Reference
<i>A. vinelandii</i>	UW136	Wild Type	Bishop <i>et al.</i> 1977
<i>A. vinelandii</i>	MV474	rhda null mutant	Colnaghi <i>et al.</i> 1996
<i>E. coli</i>	K12MG1655	Wild Type	Blattner <i>et al.</i> 1997
<i>E. coli</i>	Δ sseA6	ssea null mutant	Celestini 2001
<i>E. coli</i>	BL21(DE3)	F ⁻ dcm ompT hsdS(r _B ⁻ m _B ⁻)galA(DE3)	Studier <i>et al.</i> 1990

Table 3: Bacterial species and their characteristics.

The strains were stored in 25% glycerol at -80°C.

A. vinelandii cells were grown aerobically at 30°C in Burk's medium (0.36 mM K₂HPO₄, 0.12 mM KH₂PO₄, 0.1 mM Na₂SO₄, 1mM MgCl₂, 0.03 mM CaCl₂, 0.25 mM Na₂MoO₄, 1 mM FeNaEDTA) supplemented with sucrose 1% (w/v) in the presence (BSN) or in the absence (BS) of 14 mM ammonium acetate as nitrogen source, (Bishop *et al.* 1977).

E. coli cells were grown at 37°C using two different media: Luria Bertani Broth (LB) and M9 minimal medium (Sambrok *et al.* 1989). The LB Broth is composed by triptone (1% w/v), yeast extract (0.5%) and NaCl (1%), dissolved in water, and pH was adjusted to 7.5 using 1M NaOH. Solid medium was obtained by addition of agar (1.5%). The M9 minimal medium contained 72 mM Na₂HPO₄, 22 mM KH₂PO₄, 8.6 mM NaCl, 18.7 mM NH₄Cl, 2 mM MgSO₄, 0.1 mM CaCl₂, 0.01% thiamine and 4% solution of the appropriate carbon source (glucose or gluconate). When lactate was used as carbon source, the M9 minimal medium contained 73.5 mM K₂HPO₄ and 5.1 mM NaCl.

Sterilization of the media was carried out at 120°C for 20 min. Cells growth in liquid cultures was generally carried out under shaking (180 and 150 rpm for *E. coli* and *A. vinelandii*, respectively).

In condition of induced oxidative stress, the cells were grown up to $OD_{600nm}=0.8$ and then the cultures were treated with the following oxidative agents:

- phenazine methosulfate (PMS, 15-25 μ M final concentration) (Nachin *et al.*, 2003);
- H_2O_2 (0.2, 2 and 20 mM final concentration) (Antelmann *et al.*, 1996).

5.1.1 Plasmid vectors

The plasmids (Fig.28) for the heterologous expression of IscS and NifS in *E. coli*, (both deriving from pT7-7, kindly provided by Dean DR Lab) were:

- pDB943, used to express a full-length IscS from *A. vinelandii*; (ampicillin resistant);
- pDB551, used to express a full-length NifS from *A. vinelandii*; (ampicillin resistant).

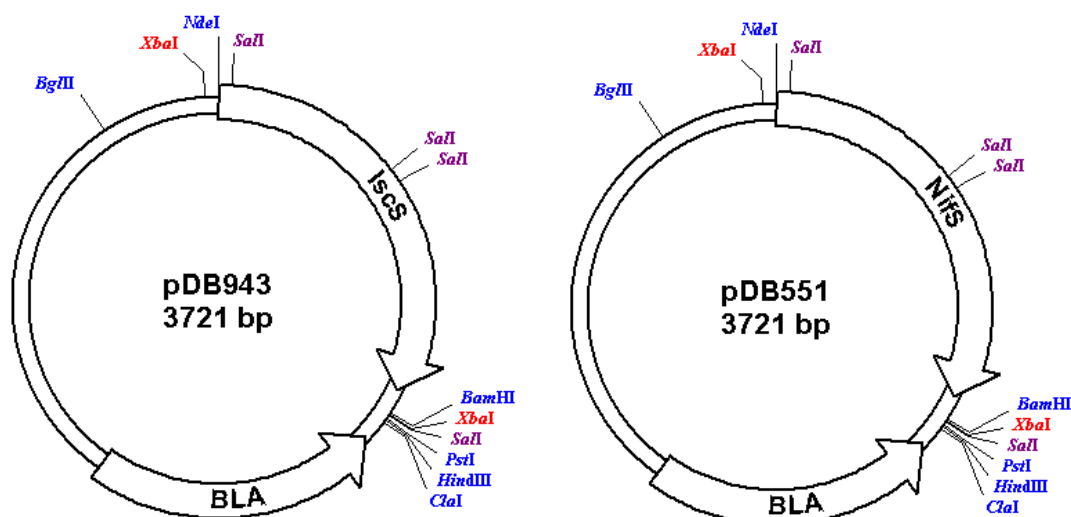


Figure 28: Plasmids for the heterologous expression in *E. coli* of IscS and NifS from *A. vinelandii*

The plasmid used to over-express RhdA in *E. coli* was pQER1, (Colnaghi *et al.*, 1996).

5.1.2 BL21(DE3) transformation

The cellular line BL21(DE3) was transformed by electroporation, a process in which high voltage (1700 volts) electric field pulses of short duration (5 ms) create temporary holes in the membrane of cells. These pores are generally large enough to allow plasmids to diffuse into the cell. Upon removal of the electric field, electrocompetent cells were resuspended in 1 ml of LB Broth and subject to a period of recovery (35° C, 45 min), the pores reseal and DNA is free to be transcribed and replicated within the cell.

5.1.3 Protein over-expression in *E. coli*

Ampicillin (100 µg/ml) was used to screen transformed strains that were plated on LB solid medium and grown overnight at 37° C. Then colonies were used to start the liquid culture and *E. coli* cells were grown up to an OD_{600 nm} =0.5. Over-expression of the proteins (RhdA, IscS and NifS) was induced by addition of 1mM isopropyl-β-D-thiogalactopyranoside (IPTG), and growth was prolonged per 4 hours. To better over-express the cysteine desulfurases, 200 µM PLP (pyridoxal-5'-phosphate) was added in the medium.

5.2 Preparation of bacterial extracts and purification of the over-expressed proteins

5.2.1 *A. vinelandii* total protein extract

A. vinelandii cells were harvested by centrifugation (3000 x g, 30 min) and after washing with Low Salt Washing Buffer (LSWB, KCl 3 mM, KH₂PO₄ 1,5 mM, NaCl 68 mM and NaH₂PO₄ 9 mM), the pellet was stored at -80°C. Frozen cells were resuspended in 50 mM Tris-HCl pH 8 containing 50 mM NaCl. After 5 sonication cycles in ice (14 amplitude microns, 30 sec), the soluble proteins (crude extract, CE) were separated by centrifugations (8000 rpm, 40 min and 12000 rpm, 40 min).

5.2.2 RhdA purification

Taking advantage of the His-tag insertion in *rhdA*, the purification was obtained by NiNTA affinity chromatography of the CE.

Unbound proteins were eluted with the equilibration buffer (50 mM Tris-HCl pH 8, 300mM NaCl). The same buffer containing glycerol 10% and imidazole 80 mM allowed the elution of the contaminant proteins. RhdA was recovered by elution with the buffer containing glycerol 10% and imidazole 300 mM (pH 6), precipitated in ammonium sulfate (75%), collected by centrifugation (8000 rpm, 40 min) and stored at -20°C.

Sulfane sulfur deprived RhdA (RhdA-SH) was obtained from the ammonium sulfate pellet resuspended in 50 mM Tris-HCl pH 8, 50 mM NaCl by treatment with 2 mM cyanide and 2 mM DTT (1 hour reaction in ice). Inactive RhdA was obtained by chemically blocking the catalytic Cys₂₃₀ with monoBromoBimane (mBBr). The ammonium sulfate pellet resuspended in 50 mM Tris-HCl pH 8, 50 mM NaCl was incubated (2h), at room temperature, in the presence of 2 mM cyanide, 2 mM DTT and 5 mM mBBr. The reaction was carried out in the dark and under continuous stirring. Either for RhdA-SH or RhdA-mBBr, the reaction mixtures were centrifuged (12000 rpm, 4° C, 10 min), and the supernatants gel-filtered using a Sepharose G25 column.

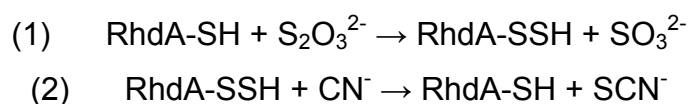
5.2.3 *A. vinelandii* cysteine desulfurases purification

The *E. coli* cells containing either pDB943 (for IscS over-expression) or pDB551 (for NifS over-expression), were harvested by centrifugation (3000 X g, 30 min), washed with LSWB and stored at -80°C. For IscS and NifS purification, frozen cells were resuspended in 50 mM Tris-HCl pH 7.5 containing 20 mM DTT. After 5 sonication cycles in ice (14 amplitude microns, 30 sec), the CE were separated by centrifugation (8000 rpm, 40 min and 12000 rpm, 40 min). The cysteine desulfurase present in the CE, (NifS or IscS), was precipitated at 45% ammonium sulfate saturation and collected by centrifugation (8000 rpm, 40 min). The pellets were resuspended in 50 mM Tris-HCl pH 7.5, 2 mM DTT buffer and gel-filtered using a Sepharose G25 column. Further purification was obtained by chromatography of the eluate from the Sepharose G25 column using a Mono Q 5/50 GL column. Purified IscS or NifS were collected and concentrated using Centricon®. The cysteine desulfurases were stored at -30°C in the presence of 20% glycerol.

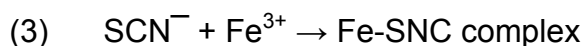
5.3 Enzyme assays

5.3.1 Thiosulfate:cyanide sulfurtransferase (TST) activity

The discontinuous method that quantifies the product thiocyanate, based on the absorbance of the ferric-thiocyanate complex (reddish brown color) at 460 nm was used to determine TST activity (Sörbo 1953; Westley, 1981). Production of SCN^- was generated in the presence of 60 mM of $\text{Na}_2\text{S}_2\text{O}_3$ and 60 mM of KCN, according to the following reactions:



The assays lasted 1 or 2 min and the reactions were stopped by addition of HCHO. Addition of the Sörbo reagent (100 g of $\text{Fe}(\text{NO}_3)_3 \times 9 \text{H}_2\text{O}$, 200 ml of 65% HNO_3 to 1 liter H_2O) allowed the formation of Fe-SNC complex ($\epsilon_{460\text{nm}} = 2890 \text{ M}^{-1} \text{ cm}^{-1}$)



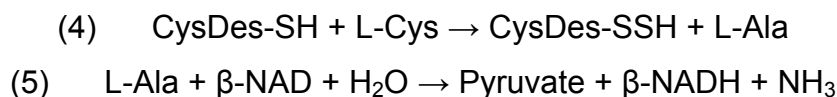
One unit (U) of activity is defined as the amount of enzyme that produces 1 μmol thiocyanate/min at 37°C.

5.3.2 Cysteine desulfurase activity assays

5.3.2.1 Alanine production

The cysteine desulfurase activity assay, in term of alanine production (Layer *et al.*, 2007), were performed in 50 mM TRIS-HCl, pH 7.5, 200 mM NaCl containing 3 mM DTT (final volume 100 μl). In the presence of 2 μM cysteine desulfurases, the reaction was started by addition of 250 μM L-cysteine and was allowed to proceed for 15 min at 27°C. After heating of the reaction mixture (99°C, 10 min), denatured proteins were removed by centrifugation

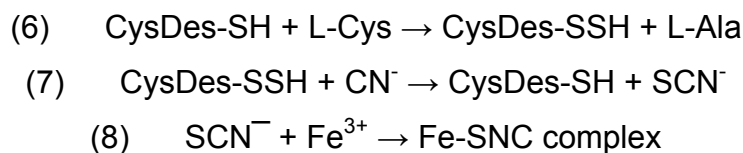
and the alanine content in the supernatant was determined by using alanine dehydrogenase reaction (Bergmeyer 1983).



Alanine formation was quantified by the absorbance at 340 nm ($\epsilon_{340\text{nm}} = 6220 \text{ M}^{-1} \text{ cm}^{-1}$) of the NADH produced during the reaction (5). One unit (U) of activity is defined as the amount of the enzyme that converts 1 μmol of L-alanine to pyruvate and NH_3 per min at 25°C.

5.3.2.2 Sulfane sulfur determination

The sulfane sulfur present the persulfurated form of the cysteine desulfurases was quantified by the absorbance of the ferric-thiocyanate complex at 460 (Sorbo 1953) according the following reactions:



The assays were carried out in the presence of 4 mM L-Cysteine. 30 mM KCN and 10 μM PLP (25°C, 15 min). One unit (U) of “activity” is defined as the amount of enzyme that produces 1 μmol thiocyanate/min at 25°C.

5.4 Spectroscopic measurements

Fluorescence measurements were performed using a LS50 instrument equipped with a thermostatic (25°C) cell holder. The excitation wavelength was 280 nm, emission spectra were recorded from 300 to 400 nm, as previously reported (Pagani *et al.*, 2000). The following formula was used to calculate the extent of RhdA persulfuration:

$$\text{RhdA-SSH, \%} = \frac{F_{\text{CN}} - F_0}{F_{\text{CN}} - F_{\text{THIO}}} \times 100$$

where F_0 is the intrinsic fluorescence ($\lambda_{\text{exc}} = 280$ nm; $\lambda_{\text{em}} = 340$ nm) of the isolated RhdA, F_{CN} and F_{THIO} the intrinsic fluorescence of the protein after cyanide and thiosulfate addition, respectively.

Sulphur transfer from cysteine desulfurases to RhdA was analyzed by a time-course fluorescence assay that monitors the changes of RhdA intrinsic fluorescence in the presence of 4 mM *L*-cysteine and 10 μ M PLP. The quenching of RhdA fluorescence was monitored in 1 ml of 50 mM Tris-HCl, 100 mM NaCl, pH 8. To obtain the complete persulfuration of RhdA, 0.5 mM $\text{Na}_2\text{S}_2\text{O}_3$ was added.

5.5 Protein-protein interactions

To study the possible in vitro interactions between RhdA and the cysteine desulfurases, two different types of chromatography were used: size-exclusion chromatography and immunoaffinity chromatography.

5.5.1 Size-exclusion chromatography

RhdA and the cysteine desulfurases, IscS or NifS, were incubated 1 h at 25°C, in the presence of 4 mM Cys and 10 µM PLP. The samples were then loaded on a Superose 12 10/300 GL column. High performance gel filtration was carried out by using TRIS-HCl 50 mM pH 8 containing NaCl 0.1 M, (Yang *et al.*, 2006).

5.5.2 Immunoaffinity chromatography

Three different types of matrix were tested: Affi-Gel Hz, CNBr-activated Sepharose 4B and HiTrap Protein A HP.

Affi-Gel Hz hydrazide gel is an agarose support which reacts with the aldehydes of oxidized carbohydrates to form hydrazone bond. The carbohydrate localized on the Fc region (heavy chain) of the antibodies anti-RhdA were oxidized with sodium m-periodate to forms aldehyde groups for specific coupling to Affi-Gel Hz following the instruction manual (Affi-Gel® Hz Immunoaffinity Kit Instruction Manual Cat. Nr 153-6060, BIORAD). *A. vinelandii* extracts were loaded into the antibody-immobilized Affi-Gel Hz column and left interact with the matrix at room temperature. After 3 hours incubation, unbound proteins were eluted using TRIS-HCl 50 mM, pH 7.4, NaCl 0.2 M. Acid elution (sodium citrate 0.15 M, pH 3) was used to recover bound proteins.

CNBr-activated Sepharose 4B was used to immobilize the anti-RhdA antibodies following the procedures described in the instruction manual (CNBr-activated Sepharose 4B Instructins 71-7086-00 AD GE Healthcare). *A. vinelandii* protein extracts were loaded on the affinity column and, after 3 hours reaction at room temperature, unbound protein were eluted using TRIS-HCl 25 mM, pH 7.4 containing NaCl 50 M. Glycine-HCl 0.1 M, pH 2.6 was used to elute the bound proteins.

HiTrap Protein A HP is a pre-packed column with Protein A Sepharose and was used to co-purify the antibodies anti-RhdA and their antigen. *A. vinelandii* protein extracts were incubated 3 hours with the antibodies anti-RhdA at room temperature, then the mixture were loaded into the column. After washing with TRIS-HCl 25 mM, pH 7.4 containing NaCl 50 mM followed by TRIS-HCl 50 mM, pH 7.4 containing NaCl 0.5 M, the anti-RhdA antibodies were co-eluted with the interacting proteins using glycine-HCl 0.1 M, pH 2.6.

5.6 Protein electrophoresis

SDS Polyacrylamide Gel Electrophoresis (SDS-PAGE) was done according to Laemmli (1970). Protein samples were denatured, in the presence of β -mercaptoethanol, by 10 min heating at 100°C in the SDS-PAGE sample buffer and loaded into SDS gels, (run was carried out at 16 mA constant x each gel). The proteins were visualized using either Coomassie Brilliant Blue or Silver Staining. Gels were digitized by a Studioscan II scanner and processed with Image MasterTM-1D Elite (Nonlinear Dynamics Ltd, Amersham Pharmacia Biotech) to quantify the protein bands.

Molecular weight markers were: β phosphorilase (97 kDa), BSA (66 kDa), egg's albumin (45 kDa), carbonic anidrase (30 kDa), trypsin inhibitor (20.1 kDa) and lisozyme (14.4 kDa)

Electrotransfer into nitrocellulose membranes was performed using the Blotting Buffer (39 mM glycine, 48 mM Tris-HCl pH 9 containing 0.03% SDS and 12% methanol). After 1 hour run (50 mA constant), the membrane was blocked 2 hours with BSA (3% w/v) in PBS buffer (15 mM NaH₂PO₄ and 150 mM NaCl, pH 7.2). The membrane was then washed with PBS containing 0.05% TWEEN 20.

The first incubation was in presence of anti-RhdA antibodies diluted 1:2500, the second one in the presence of anti-rabbit antibodies peroxidase conjugated 1:3000 (Biorad). Staining was performed by using 4-cloronaphtol (0.4 mg/ml), H₂O₂ 0.02% and 10% of methanol in PBS.

6.References

- Agar JN, Krebs C, Frazzon J, Huynh BH, Dean DR, Johnson MK. IscU as a scaffold for iron-sulfur cluster biosynthesis: sequential assembly of [2Fe-2S] and [4Fe-4S] clusters in IscU. *Biochemistry* 39: 7856–7862, (2000a)
- Agar JN, Yuvaniyama P, Jack RF, Cash VL, Smith AD, Dean DR, Johnson MK. Modular organization and identification of a mononuclear iron-binding site within the NifU protein. *Journal of Biological Inorganic Chemistry* 5: 167–177, (2000b)
- Agar JN, Zheng L, Cash VL, Dean DR, Johnson MK. Role of the IscU protein in iron-sulfur cluster biosynthesis: IscS mediated assembly of a [Fe₂S₂] cluster in IscU. *Journal of the American Chemical Society* 122: 2136–2137, (2000c)
- Antelmann H, Engelmann S, Schimid R, Hecker M. General and oxidative stress response in *Bacillus subtilis*: cloning, expression and mutation of the alkyl hydroperoxide reductase operon. *Journal of Bacteriology* 178: 6571-6578, (1996)
- Bächli B and Kornberg HL. Utilization of gluconate by *Escherichia coli*. A role of adenosine 3':5'-cyclic monophosphate in the induction of gluconate catabolism. *Journal of Biochemistry* 150: 23-128, (1975)
- Begley TP, Xi J, Kinsland C, Taylor S, McLafferty F. The enzymology of sulfur activation during thiamine and biotin biosynthesis. *Current Opinion in Chemical Biology* 3: 623–629, (1999)
- Beinert H. A tribute to sulphur. *European Journal of Biochemistry* 267:5657-5664, (2000)
- Bergmeyer HU. *Methods of Enzymatic Analysis*, 2nd edition, Vol.1, 427, (1983)
- Bishop PE and Brill WJ. Genetic analysis of *Azotobacter vinelandii* mutant strain enable to fix nitrogen, *Journal of Bacteriology* 130: 954-956, (1977).
- Blattner FR, Plunkett G III, Bloch CA, Perna NT, Burland V, Riley M, Collado-Vides J, Glasner JD, Rode CK, Mayhew GF, Gregor J, Davis NW, Kirkpatrick HA, Goeden MA, Rose DJ, Mau B and Shao Y. The complete genome sequence of *Escherichia coli* K-12. *Science* 277: 1453-1474, (1997).
- Bordo D, Colnaghi R, Deriu D, Carpen A, Storici P, Pagani S and Bolognesi M. Crystallization and preliminary crystallographic investigations of rhodanese from *Azotobacter vinelandii*. *Acta Crystallographica sect. D*, 55: 1471-1473, (1999)
- Bordo D, Deriu D, Colnaghi R, Carpen A, Pagani S and Bolognesi M. The crystal structure of a sulfurtransferase from *Azotobacter vinelandii* highlights the evolutionary relationship between the rhodanese and phosphatase enzyme families. *Journal of Molecular Biology* 298: 691–704, (2000).

- Bordo D, Forlani F, Spallarossa A, Colnaghi R, Carpen A, Bolognesi M and Pagani S. A persulfurated cysteine promotes active-site reactivity in *Azotobacter vinelandii* rhodanese. *Biological Chemistry* 382: 245-1252, (2001).
- Bordo D and Bork P. The rhodanese/Cdc25 phosphatase superfamily: sequence, structure and function relation. *EMBO reports* 3: 741-746, (2002).
- Celestini F, Knockout del gene *sseA* di *Escherichia coli*: uno strumento per lo studio del ruolo biologico di proteine "sulfurtransferase-related.", Tesi di Laurea in Biotecnologie Agrarie Vegetali, (2001).
- Cereda A, Forlani F, Iametti S, Bernhardt R, Ferranti P, Picariello G, Pagani S and Bonomi F. Molecular recognition between *Azotobacter vinelandii* rhodanese and a sulfur acceptor protein. *Biological Chemistry* 384: 1473-1481, (2003).
- Cereda A, Carpen A, Picariello G, Iriti M, Faoro F, Ferranti P and Pagani S. Effects of the deficiency of the rhodanese-like protein RhdA in *Azotobacter vinelandii*. *FEBS Letters* 581: 1625-1630, (2007)
- Colnaghi R, Pagani S, Kennedy C and Drummond M. Cloning, sequence analysis and overexpression of the rhodanese gene of *Azotobacter vinelandii*. *European Journal of Biochemistry* 236: 240-248, (1996).
- Colnaghi R, Cassinelli G, Drummond M, Forlani F and Pagani S. Properties of the *Escherichia coli* rhodanese-like protein SseA: contribution of the active-site residue Ser240 to sulfur recognition. *FEBS Letters* 500: 153–156, (2001).
- Egan S, Fliege R, Tong S, Shibata A, Wolf RE Jr and Conway T. Molecular characterization of the Entner-Doudoroff pathway in *Escherichia coli*: sequence analysis and localization of promoters for the *edd-eda* operon. *Journal of Bacteriology* 174: 4638-4646, (1992)
- Esnousf BM An extensively modified version of MOLSCRIPT that includes greatly enhanced coloring capabilities. *Journal of Molecular Graphics* 15: 138, (1997).
- Evans DJ, Jones R, Woodley PR, Wilborn JR, Robson RL. Nucleotide sequence and genetic analysis of the *Azotobacter chroococcum* *nifUSVWZM* gene cluster, including a new gene (*nifP*) which encodes a serine acetyltransferase. *Journal of Bacteriology* 173: 5457–69, (1991).
- Fauman EB, Cogswell JP, Lovejoy B, Rocque WJ, Holmes W, Montana VG, Piwnicka-Worms H, Rink M and Saper MA. Crystal structure of the catalytic domain of the human cell cycle control phosphatase, Cdc25A. *Cell* 93: 617–625, (1998).

-
- Felsenstein J. PHYLIP. Phylogeny Inference Package (Version 3.2). *Cladistics* 5: 164–166, (1989).
 - Fontecave M, Ollaignier de Choudens S, Py B and Barras F. Mechanisms of iron-sulfur cluster assembly: the SUF machinery. *Journal of Biological Inorganic Chemistry* 10: 713–721, (2005)
 - Forlani F, Carpen A, Pagani S. Evidence that elongation of the catalytic loop of the *Azotobacter vinelandii* rhodanese changed selectivity from sulphur- to phosphate-containing substrates. *Protein Engineering* 16: 1-5, (2003).
 - Forlani F, Cereda A, Freuer A, Nimitz M, Leimkühler S, Pagani S. The cysteine-desulfurase IscS promotes the production of the rhodanese RhdA in the persulfurated form. *FEBS Letters* 579: 6786-6790, (2005).
 - Fu W, Jack RF, Morgan TV, Dean DR, Johnson MK. nifU gene product from *Azotobacter vinelandii* is a homodimer that contains two identical [2Fe-2S] clusters. *Biochemistry* 33: 13455–13463, (1994)
 - Fuhrman LK, Wanker A, Nickerson KW and Conway T. Rapid accumulation of intracellular 2-keto-3-deoxy-6-phosphogluconate in an Entner-Doudoroff aldolase mutant results in bacteriostasis. *FEMS Microbiology Letters* 159: 261-266, (1998)
 - Hama H, Kayahara T, Ogawa W, Tsuda M and Tsuchiya T. Enhancement of Serine-Sensitivity by a Gene Encoding Rhodanese-Like Protein in *Escherichia coli*. *Journal of Biochemistry* 115: 1135-1140, (1994)
 - Hofmann K, Bucher P and Kajava AV. A model of Cdc25 phosphatase catalytic domain and Cdk-interaction surface based on the presence of a rhodanese homology domain. *Journal of Molecular Biology* 282: 195–208, (1998).
 - Jacobson MR, Cash VL, Weiss MC, Laird NF, Newton WE, Dean DR. Biochemical and genetic analysis of the *nifUSVWZM* cluster from *Azotobacter vinelandii*. *Molecular Genetics and Genomics* 219: 49–57, (1989)
 - Kambampati R and Lauhon CT. IscS Is a Sulfurtransferase for the *in Vitro* Biosynthesis of 4-Thiouridine in *Escherichia coli* tRNA. *Biochemistry* 38: 16561-16568, (1999)
 - Kaiser JT, Clausen T, Bourenkow GP, Bartunik HD, Steinbacher S, Huber R. Crystal structure of a NifS-like protein from *Thermotoga maritima*: implications for iron sulphur cluster assembly. *Journal of Molecular Biology* 297: 451–464, (2000)
 - Kato S, Mihara H, Kurihara T, Takahashi Y, Tokumoto U, Yoshimura T, Esaki N. Cys-328 of IscS and Cys-63 of IscU are the sites of disulfide bridge formation in a covalently bound IscS/IscU complex: implications for the mechanism of iron-sulfur cluster assembly.

Proceedings of the National Academy of Sciences of the United States of America 99: 5948-5952, (2002).

- Kessler D. Enzymatic activation of sulphur for incorporation into biomolecules in prokaryotes, *FEMS Microbiology Review* 30: 825-840, (2006)
- Keyse SM and Ginsburg M. Amino acid sequence similarity between CL100, a dual specific MAP kinase phosphatase and Cdc25. *Trends in Biochemical Sciences* 18: 377–378, (1993).
- Kraulis PJ. MOLSCRIPT: a program to produce both detailed and schematic plots of protein structures. *Journal of Applied Crystallography* 24: 946-950, (1991).
- Ikeuchi Y, Shigi N, Kato J, Nishimura A and Suzuki T. Mechanistic insights into sulfur relay by multiple sulfur mediators involved in thiouridine biosynthesis at tRNA wobble positions. *Molecular Cell* 21: 97-108, (2006)
- Laemmli UK. Cleavage of structural proteins during the assembly of the head of bacteriophage T4. *Nature* 227: 680-685, (1970)
- Layer G, Aparna Gaddam S, Ayala-Castro CN, Ollagnier-de Choudens S, Lascoux D, Fontecave M, Outten FW. SufE transfer sulfur from SufS to SufB for iron-sulfur cluster assembly. *Journal of Biological Chemistry* 282: 13342-13350, (2007)
- Leibrecht I, Kessler D. A novel L-cysteine/cystine C-S lyase directing [2Fe-2S] cluster formation of *Synechocystis* ferredoxin. *Journal of Biological Chemistry* 272: 10442–10447, (1997)
- Luo G and Horowitz PM. The sulfurtransferase activity and structure of rhodanese are affected by site-directed replacement of Arg-186 or Lys-249. *Journal of Biological Chemistry* 269: 8220-8225, (1994).
- Marquet A. Enzymology of carbon-sulfur bond formation. *Current Opinion in Chemical Biology* 5: 541–549, (2001)
- Matthies A, Rajagopalan KV, Mendel RR and Leimkühler S. Evidence for the physiological role of a rhodanese-like protein for the biosynthesis of the molybdenum cofactor in humans. *Proceedings of the National Academy of Sciences of the United States of America* 101: 5946-5951, (2004)
- Matthies A, Nimtz M and Leimkuhler S. Molybdenum Cofactor Biosynthesis in Humans: Identification of a Persulfide Group in the Rhodanese-like Domain of MOCS3 by Mass Spectrometry. *Biochemistry*, 44: 7912-7920, (2005)
- Merrit EA and Murphy MEP. Raster3d, a program for photorealistic molecular graphics. *Acta Crystallographica sect. D*, 50: 869-873, (1994).

-
- Mihara H and Esaky N. Bacterial cysteine desulfurases: their function and mechanisms. *Applied Microbiology and Biotechnology* 60: 12-23, (2002)
 - Mueller EG. Trafficking in persulfides: delivering sulfur in biosynthetic pathways. *Nature Chemical Biology* 4: 185-194, (2006)
 - Nachin L, Loiseau L, Expert D, Barras F. SufC: an unorthodox cytoplasmic ABC/ATPase required for [Fe-S] biogenesis under oxidative stress. *The EMBO Journal* 22: 427-437, (2003)
 - Nagahara N, Okazaki T and Nishino T. Cytosolic mercaptopyruvate sulfurtransferase is evolutionarily related to mitochondrial rhodanese. *Journal of Biological Chemistry* 270: 16230–16235, (1995).
 - Nagahara N and Nishino T. Role of amino acid residues in the active site of rat liver mercaptopyruvate sulfurtransferase. cDNA cloning, overexpression, and site-directed mutagenesis. *Journal of Biological Chemistry* 271: 27395–27401, (1996).
 - Nagahara N, Ito T and Minami N. Mercaptopyruvate sulfurtransferase as a defense against cyanide detoxification: molecular properties and mode of detoxification. *Histology and Hystopathology* 14: 1277-1286, (1999).
 - Nakamura M, Saeki K, Takahashi Y. Hyperproduction of recombinant ferredoxins in *Escherichia coli* by coexpression of the ORF1-ORF2-iscS-iscU-iscA-hscB-hscA-fdx-ORF3 gene cluster. *Journal of Biochemistry (Tokyo)* 126: 10–18, (1999)
 - Pagani S, Forlani F, Carpen A, Bordo D and Colnaghi R. Mutagenic analysis of Thr-232 in rhodanese from *Azotobacter vinelandii* highlighted the differences of this prokaryotic enzyme from the known sulfurtransferases. *FEBS Letters* 472: 307-311, (2000).
 - Palenchar PM, Buck CJ, Cheng H, Larson TJ and Mueller EG. Evidence that ThiI, an enzyme shared between thiamin and 4-thiouridine biosynthesis, may be a sulfurtransferase that proceeds through a persulfide intermediate. *Journal of Biological Chemistry* 275: 8283–8286, (2000).
 - Papenbrock J and Schmidt A. Characterization of two sulfurtransferase isozymes from *Arabidopsis thaliana*. *European Journal of Biochemistry* 267: 5571–5579, (2000).
 - Peekhaus N and Conway T. What's for dinner?: Entner-Doudoroff metabolism in *Escherichia coli*. *Journal of Bacteriology* 180: 3495-3502, (1998)
 - Ploegman JH, Drent G, Kalk KH, Hol WGJ, Heinrikson RL, Kleim P, Weng L, Russel J. The covalent and tertiary structure of bovine liver rhodanese. *Nature* 273: 124-129, (1978).

-
- Porco A, Peekhaus N, Bausch C, Tong S, Isturiz T and Conway T. Molecular genetic characterization of the *Escherichia coli* *gnT* gene of Gntl, the main system for gluconate metabolism. *Journal of Bacteriology* 179: 1584-1590, (1997)
 - Ray WK, Zeng G, Potters MB, Mansuri AM and Larson TJ. Characterization of a 12-kilodalton rhodanese encoded by *glpE* of *Escherichia coli* and its interaction with thioredoxin. *Journal of Bacteriology* 182: 2277-2284, (2000).
 - Reynolds RA, Yem AW, Wolfe CL, Deibel MR Jr, Chidester CG and Watenpaugh KD. Crystal structure of the catalytic subunit of Cdc25B required for G₂/M phase transition of the cell cycle. *Journal of Molecular Biology* 293: 559–568, (1999).
 - Sambrook J, Fritsch EF and Maniatis T. Molecular cloning: a laboratory manual, *Cold Spring Harbour Laboratory Press*, 2nd edition ed., (1989).
 - Schultz J, Milpetz F, Bork P and Ponting CP. SMART, a simple modular architecture research tool: identification of signaling domains. *Proceedings of the National Academy Sciences* 95: 5857–5864, (1998).
 - Schwartz CJ, Djaman O, Imlay JA, Kiley PJ. The cysteine desulfurase, IscS, has a major role in in vivo Fe-S cluster formation in *Escherichia coli*. *Proceeding of the National Academy of Sciences USA* 97: 9009–9014, (2000)
 - Skovran E, Downs DM. Metabolic defects caused by mutations in the *isc* gene cluster in *Salmonella enterica* Serovar Typhimurium: implications for thiamine synthesis. *Journal of Bacteriology* 182: 3896–3903(2000)
 - Smith AD, Agar JN, Johnson KA, Frazzon J, Amster IJ, Dean DR, Johnson MK. Sulfur transfer from IscS to IscU: the first step in iron-sulfur cluster biosynthesis. *Journal of the American Chemical Society* 123: 11103–11104, (2001)
 - Sorbo BH. On the substrate specificity of rhodanese. *Acta Chemica Scandinavica* 7: 1137–1145, (1953)
 - Spallarossa A, Donahue J, Larson TJ, Bolognesi M and Bordo D. *Escherichia coli* GlpE is a prototype sulfurtransferase for the single-domain rhodanese homology superfamily. *Structure* 9: 1117–1125, (2001).
 - Spallarossa A, Forlani F, Carpen A, Armirotti A, Pagani S, Bolognesi M and Bordo D. The “Rhodanese” Fold and Catalytic Mechanism of 3-Mercaptopyruvate Sulfurtransferases: Crystal Structure of SseA from *Escherichia coli*. *J. Mol. Biol.* 335: 583-593, (2004).
 - Studier FW, Rosenberg AH, Dunn JJ and Dubendorff JW. Use of T7 RNA polymerase to direct expression of cloned genes. *Methods Enzymology* 185: 60-89, (1990).

-
- Takahashi Y, Nakamura M. Functional assignment of the ORF2-*iscS-iscU-iscA-hscB-hscA-fdx*-ORF3 gene cluster involved in the assembly of Fe-S clusters in *Escherichia coli*. *Journal of Biochemistry* (Tokyo) 126: 917–926, (1999)
 - Tatusov RL, Galperin MY, Natale DA and Koonin EV. The COG database: a tool for genome-scale analysis of protein functions and evolution. *Nucleic Acids Research*, 33–36, (2000).
 - Thompson JD, Gibson TJ, Plewniak F, Jeanmougin F and Higgins DG. The ClustalX windows interface: flexible strategies for multiple sequence alignment aided by quality analysis tools. *Nucleic Acids Research* 24: 4876–4882, (1997).
 - Tokumoto U, Takahashi Y. Genetic analysis of the *isc* operon in *Escherichia coli* involved in the biogenesis of cellular iron-sulfur proteins. *Journal of Biochemistry* (Tokyo) 130: 63–71, (2001)
 - Tong S, Porco A, Isturiz T and Conway T. Cloning and molecular characterization of the *Escherichia coli* *gntR*, *gntK* and *gntU* genes of Gntl, the main system for gluconate metabolism. *Journal of Bacteriology* 178: 3260-3269, (1996)
 - Toohey JI. Sulfane sulphur in biological system: a possible regulatory role. *Biochemistry Journal* 264: 625-632, (1989)
 - Urbina HD, Silberg JJ, Hoff KG and Vickery LE. Transfer of sulfur from IscS to IscU during Fe/S Cluster assembly. *Journal of Biological Chemistry* 276: 44521-44526, (2001).
 - Westley J. Sulfane-transfer catalysis by enzymes. *Bioorganic Chemistry* 1: 371-390, (1977).
 - Westley J. Thiosulfate: cyanide sulfurtransferase (Rhodanese). *Methods in Enzymology* 77: 285–291, (1981).
 - Westley J, Adler H, Westley L and Nishida C. The sulfurtransferases. *Fundamental and Applied Toxicology* 3: 377-382, (1983).
 - Yang J, Bitoun JP, Ding H. Interplay of IscA and IscU in biogenesis of iron-sulfur clusters, *Journal of Biological Chemistry* 281: 27956-27963, (2006).
 - Yuvaniyama P, Agar JN, Cash VL, Johnson MK, Dean DR. NifS-directed assembly of a transient [2Fe-2S] cluster within the NifU protein. *Proceeding of the National Academy of Sciences USA* 97: 599–604, (2000)
 - Zheng L, White RH, Cash VL, Jack RF, Dean DR. Cysteine desulfurase activity indicates a role for NIFS in metallocluster biosynthesis. *Proceeding of the National Academy of Sciences USA* 90: 2754–2758, (1993)

- Zheng L, White RH, Cash VL, Dean DR. Mechanism for the desulfurization of L-cysteine catalyzed by the *nifS* gene product. *Biochemistry* 33: 4714–4720, (1994)
- Zheng L, Cash VL, Flint DH and Dean DR. Assembly of Iron-Sulfur Clusters. Identification of an *iscSUA-hscBA-fdx* gene cluster from *Azotobacter vinelandii*. *Journal of Biological Chemistry* 273: 13264-13272, (1998).